Journal of Medicinal Chemistry

ARTICLE

pubs.acs.org/jmc

Discovery of the Macrocycle 11-(2-Pyrrolidin-1-yl-ethoxy)-14, 19-dioxa-5,7,26-triaza-tetracyclo[19.3.1.1(2,6).1(8,12)]heptacosa-1(25),2(26),3,5,8,10,12(27),16,21,23-decaene (SB1518), a Potent Janus Kinase 2/Fms-Like Tyrosine Kinase-3 (JAK2/FLT3) Inhibitor for the Treatment of Myelofibrosis and Lymphoma

Anthony D. William,* Angeline C.-H. Lee, Stéphanie Blanchard, Anders Poulsen, Ee Ling Teo, Harish Nagaraj, Evelyn Tan, Dizhong Chen, Meredith Williams, Eric T. Sun, Kee Chuan Goh, Wai Chung Ong, Siok Kun Goh, Stefan Hart, Ramesh Jayaraman, Mohammed Khalid Pasha, Kantharaj Ethirajulu, Jeanette M. Wood, and Brian W. Dymock

S*BIO Pte. Ltd., 1 Science Park Road, #05-09, The Capricorn, Singapore Science Park II, Singapore 117528

Supporting Information

ABSTRACT: Discovery of the activating mutation V617F in Janus Kinase 2 ($JAK2^{V617F}$), a tyrosine kinase critically involved in receptor signaling, recently ignited interest in JAK2 inhibitor therapy as a treatment for myelofibrosis (MF). Herein, we describe the design and synthesis of a series of small molecule 4-aryl-2-aminopyrimidine macrocycles and their biological evaluation against the JAK family of kinase enzymes and FLT3. The most promising leads were assessed for their in vitro ADME properties culminating in the discovery of **21c**, a potent JAK2 (IC_{50} = 23 and 19 nM for $JAK2^{WT}$ and $JAK2^{V617F}$, respectively) and FLT3 (IC_{50} = 22 nM) inhibitor with selectivity against JAK1 and JAK3 (IC_{50} = 1280 and 520 nM, respectively). Further profiling of **21c** in preclinical species and mouse xenograft and allograft models is described. Compound **21c** (SB1518) was selected as a development candidate and progressed into clinical trials where it is currently in phase 2 for MF and lymphoma.

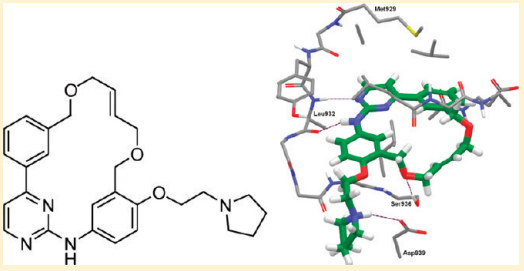

INTRODUCTION

The Janus family of kinases (JAK1, JAK2, JAK3, and TYK2) are intracellular nonreceptor tyrosine kinases that transduce cytokine-mediated signals via the JAK-STAT (signal transducer and activator of transcription) pathway and hence play an important role in the control of cell proliferation, cell differentiation, and survival.[1,2] In 2005, the discovery of the V617F mutation in JAK2 ($JAK2^{V617F}$) catalyzed significant efforts in our laboratories to bring a new small molecule JAK2 inhibitor therapy to the clinic for the treatment of a wide spectrum of hematological malignancies, particularly the myeloproliferative neoplasms (MPNs) and lymphoma.[3−7] The MPNs are a spectrum of poorly treated diseases including polycythemia vera (PV), essential thrombocythemia (ET), and primary, post-PV, and post-ET myelofibrosis (MF). MF is the most serious disease with the most severe patients having a life expectancy of between 1.5 to 5 years. The MF disease course is characterized by symptomatic splenomegaly, progressive anemia leading to fatigue, and severe constitutional symptoms including night sweats, fever, bleeding, bone pain, and frequent infections.[8] Inhibition of the JAK-STAT signaling pathways[9] in MF patients has given encouraging initial responses in recent clinical trials,[10−12] and **21c** (SB1518) described herein, has demonstrated an ability to reduce splenomegaly and improve symptoms in phase 1 and 2 clinical trials in MF patients.[13−15]

Rationale for use of JAK2 inhibitors in lymphoma is supported by a number of studies: activation of wild-type JAK2 in lymphoma cells by a mutation in the SOCS-1 gene (suppressor of cytokine signaling); discovery that a high level of a micro-RNA species targeting JAK2 (miR-135a) correlates with a favorable prognosis in classical Hodgkin lymphoma patients; and increased JAK2 gene expression in a number of lymphoma subtypes.[16−19] Furthermore, JAK2 has been implicated in inflammatory disease such as rheumatoid arthritis and psoriasis with encouraging initial clinical data.[20,21]

Selectivity for JAK2 over JAK3 was strongly desirable due to the reported immunosuppressive effects of inhibiting JAK3. Deficient JAK3 signaling in humans and mice causes severe combined immunodeficiency (SCID).[22] The effects of adding JAK1 and/or TYK2 activity to a JAK2 inhibitor are still not well understood.

Overexpression and activating mutations of receptor tyrosine kinases (RTKs) are known to be involved in the pathophysiology

Received: March 21, 2011
Published: May 23, 2011

of diverse human cancers. Further to JAK-STAT driven disease, we sought to broaden the potential application of a JAK2 inhibitor by refining additional RTK activity discovered in our leads. FLT3 (fms-like tyrosine kinase-3), a class III RTK, is the most frequently mutated gene in acute myeloid leukemia (AML) and plays an important role in the maintenance, growth, and development of hematopoietic and nonhematopoietic cells. Mutations of the FLT3 receptor can lead to the development of AML.[23−27] Hence, we were attracted to the potential of a JAK2/FLT3 combined inhibitor profile. As MF, lymphoma, and AML continue to present as unmet medical needs in hematology, JAK2/FLT3 inhibitor therapy could offer new hope for the development of a safe and effective therapy.

At the time of the first reports of the $JAK2^{V617F}$ mutation,[4−6] we were engaged in a search for novel kinase inhibitor motifs. We were evaluating a series of compounds which exhibited a unique kinase inhibitory spectrum with JAK2 and FLT3 inhibition being prominent. Rationale for JAK2 inhibitor therapy in the MPNs was strengthening, and encouraged by the additional desirable FLT3 activity we were seeing in our leads, we focused our attention on the rapid identification of a clinical candidate which would meet the desired requirements for MF and lymphoma therapy with potential for activity in other JAK2 and FLT3-driven diseases: potent and selective JAK2/FLT3 inhibition with an excellent safety profile and oral daily dosing. Herein, we describe the discovery and structure−activity relationship (SAR) of a series of small molecule macrocycles culminating in the identification of **21c**, the compound that we selected for preclinical development and then progressed into clinical trials. Compound **21c** is showing clinical benefit in patients with MF and lymphoma with many patients remaining on therapy in ongoing phase 1 and 2 trials in these indications.[28]

CHEMISTRY

In-house library screening revealed compound **1** which showed broad kinase inhibition with reasonable activity in cell lines tested; however, these rather ubiquitous pyrimidine-based motifs are heavily patented with very narrow possibilities for developing proprietary compounds.[29] We envisioned that by connecting the open ends of **1**, to form macrocycles **2**, the binding mode to the kinase hinge region is not compromised (Figure 1). Thus, we embarked on the synthesis of small molecule macrocycles by exploiting the powerful ring-closing metathesis (RCM) reaction as a synthetic tool.[30−32] We were inspired by macrocyclic natural products which, although usually complex and difficult to synthesize, have evolved to specifically interact with biological systems in ways not easily achievable with the much simpler small molecule compounds found in screening libraries.[33−35] It seemed attractive to us to explore the potential for diverse but specific functionalization possible within the ring structure of **2**, conformationally defined by the semirigid arrangement of the A, B, and C rings. Whereas open chain compounds will adopt energetically favorable conformations that are not necessarily complementary to the target binding site, the ability to position a chosen group at a desired point in space with limited conformational freedom using a constrained macrocyclic structure could have benefits leading to greater specificity between kinases. The choice of initial linkers, Z, was driven by synthetic concerns and our desire to avoid very lipophilic and flexible linkers of straight carbon chains which would dramatically increase log *P* and likely be vulnerable to phase 1 metabolism. Solubility and metabolic stability were primary concerns from the early stages;

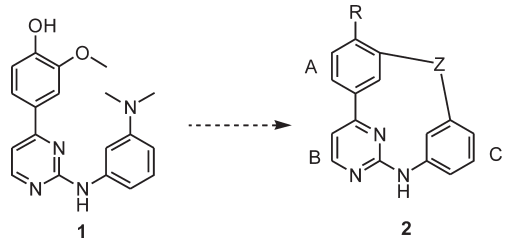

Figure 1. Inception of macrocyclization from an in-house library screening hit.

therefore, linkers with some hydrophilic character (use of oxygen atoms) and not containing any groups known to be rapidly metabolized were prioritized.

Synthesis of the macrocycles is made possible by taking advantage of the RCM reaction pioneered by Grubbs. Synthesis of the precursors for RCM was achieved by the coupling of the two halves of the molecules via acidic displacement between the chloropyrimidines and anilines.[36] In general, RCM of the dienes was achieved by employing either Grubbs second generation catalyst ($(C_{46}H_{65}Cl_2N_2PRu)$: [1,3-bis(2,4,6-trimethylphenyl)-2-imidazolidinylidene]dichloro(phenylmethylene)(tricyclohexylphosphine)ruthenium) or Zhan-1B catalyst ($(RuCl_2[C_{21}H_{26}N_2][C_{12}H_{17}NO_3S])$: 1,3-Bis(2,4,6-trimethylphenyl)-4,5-dihydroimidazol-2-ylidene[2-(i-propoxy)-5-(*N*,*N*-dimethylaminosulfonyl)phenyl]methyleneruthenium(II) dichloride).[37,38] All products were isolated as inseparable mixtures of approximately 85:15 *trans*:*cis* double bond geometry. Scheme 1 illustrates the synthetic routes for compounds **16a**−**f**.

Left-hand fragments were constructed by Suzuki coupling of commercially available 2,4-dichloropyrimidine (**3a**) and boronic acids **4a**−**b** affording the corresponding biaryl alcohols **5a**−**b** (Scheme 1).[39,40] Alkylation of the alcohols was achieved either under phase transfer conditions with allyl bromide, giving allylethers **6a**−**b**, or with cesium carbonate assisted displacement with 4-bromo-but-1-ene furnishing homoallyl ether, **7**.[41,42]

Because of their diversity, right-hand fragments were prepared using a wide variety of methods, as illustrated in Schemes 1 and 2. Commercially available alcohols **10a**−**b** (Scheme 1) were alkylated as described above by either allyl bromide or 4-bromo-but-1-ene to produce the corresponding **11a**−**b** and **13**, respectively. Iron-assisted reduction of the nitro group gave key anilines **12a**−**b** and **14**, respectively, in good to excellent yields.[43] Precursors of the RCM reaction, dienes **15a**−**e**, were prepared in moderate yield from coupling of Suzuki products **6a**−**b** and **7** and anilines **12a**−**b** and **14** in the presence of HCl under reflux conditions. Macrocyclization of **15a**−**e** proceeded efficiently in the presence of Grubbs second generation catalyst with hydrochloric acid as an additive to afford products **16a**−**f** in moderate yields.

Sequences (1−8) in Scheme 2 show the synthetic routes to obtain **12c**−**i**. The displacement reaction of **8b** with corresponding secondary amines afforded **9a**−**d** in quantitative yields. Alkylation of **8c**−**d** proceeded smoothly with 1,2-dichloroethane to afford **9e**−**f**.[44] Benzaldehydes **9a**−**f** were efficiently reduced to the corresponding benzylic alcohols **10c**−**h** using sodium borohydride. By employing phase transfer conditions with allyl bromide, the alkylated intermediates were then reduced via the aforementioned iron conditions to afford anilines **12c**−**h** in good to excellent yields. Aniline **12i** was prepared by alkylation of the benzylic alcohol **18** using

Scheme 1[a]

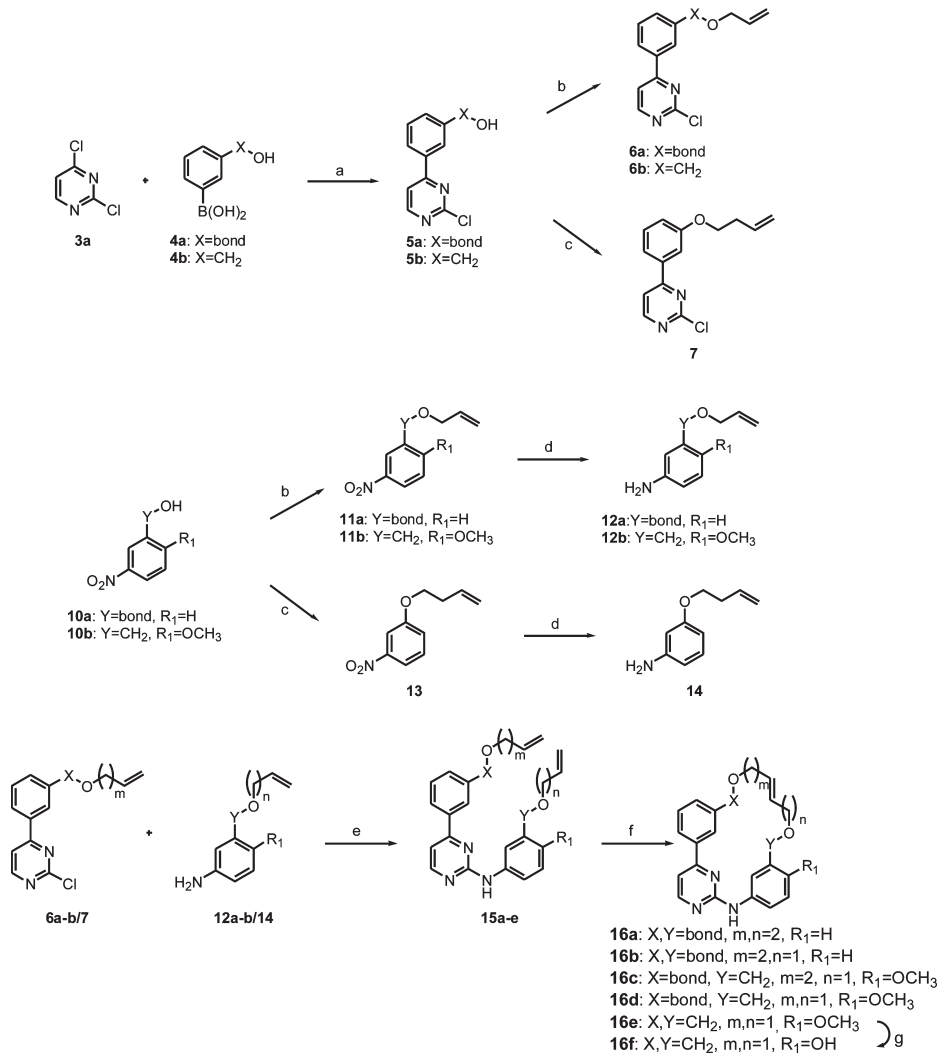

[a] Reactions and conditions: (a) $Pd(PPh_3)_4$, Na_2CO_3, 1,2-dimethoxyethane, water, 80 °C, 52−64%. (b) Allyl bromide, KOH, $TBAHSO_4$, CH_2Cl_2, rt, 38−68%. (c) 4-Bromobut-1-ene, $CsCO_3$, DMF, 40 °C, 52−64%. (d) Fe powder, NH_4Cl, EtOH, water, 80 °C, 71−96%. (e) 4 M HCl, *n*-butanol, 80−100 °C, 21−56%. (f) Grubbs second generation catalyst, HCl, CH_2Cl_2, 40−45 °C, 43−51%. (g) NaSEt, DMF, 120 °C, 30%.

phase transfer conditions. Reduction of both nitro groups gave bis-aniline **20**, which was monoprotected using Fmoc-Cl affording a quantitative yield of **12i**. Phenol **16f** was obtained though demethylation of **16e** using NaSEt.[45]

Biaryl **6b** underwent chloride displacement with anilines **12c**−**f** to furnish the respective dienes that were macrocyclized with either Grubbs second generation or Zhan-1B catalyst to afford macrocyles **17a**,**b**,**d**, and **h** in moderate yield. Compound **17c** was obtained via the removal of the Boc group from **17b**. The free amine on the piperazine ring was further derivatized by alkylation, acetylation, and sulfonylation to afford **17e**−**g**, respectively, with moderate yields. The intermediate **21a**, formed from coupling of **6b** and **12g** under reflux conditions in the presence of *n*-butanol, was further derivatized by displacement reactions with various secondary amines employing microwave conditions in DMA solvent, affording the more soluble products **21b**−**f**. Similarly, **21 h**−**i** were obtained from **21g** using the same displacement method. The intermediate **21g** was made in moderate yield by the coupling of *meta*-aniline **12h** and **6b**. Compounds **21k**−**l** were prepared first by basic removal of the Fmoc group from **21j**, prepared as described for **21g**, followed by amidation with 3-diethylamino-propionic acid (sequence 8 in Scheme 2).

Scheme 3 illustrates the synthetic route toward the preparation of diversely substituted compounds **22a**−**g**. Commercially available **8c** and **8e** were subjected to the aforementioned alkylation conditions with 1,2-dichloroethane, followed by $NaBH_4$ reduction and phase transfer allylation with allyl bromide to give **11g** and **11i**, respectively. Pyrrolidine displacement gave **11j**−**k**, which were then reduced to the anilines **12j**−**k** in excellent yields.[46] The right-hand fragments were obtained from different commercially available pyrimidines **3a**−**c** and boronic acids **4b**−**f**. Following standard Suzuki couping, aldehydes **5d** and **5h** and ester **5f** were readily reduced to the corresponding benzyl alcohols, which were alkylated using phase transfer conditions with allyl bromide to give **6b**−**h** in moderate yields. Compounds **22a**−**g** were then prepared using the above-described displacement and RCM.

dx.doi.org/10.1021/jm200326p |*J. Med. Chem.* 2011, 54, 4638–4658

Scheme 2[a]

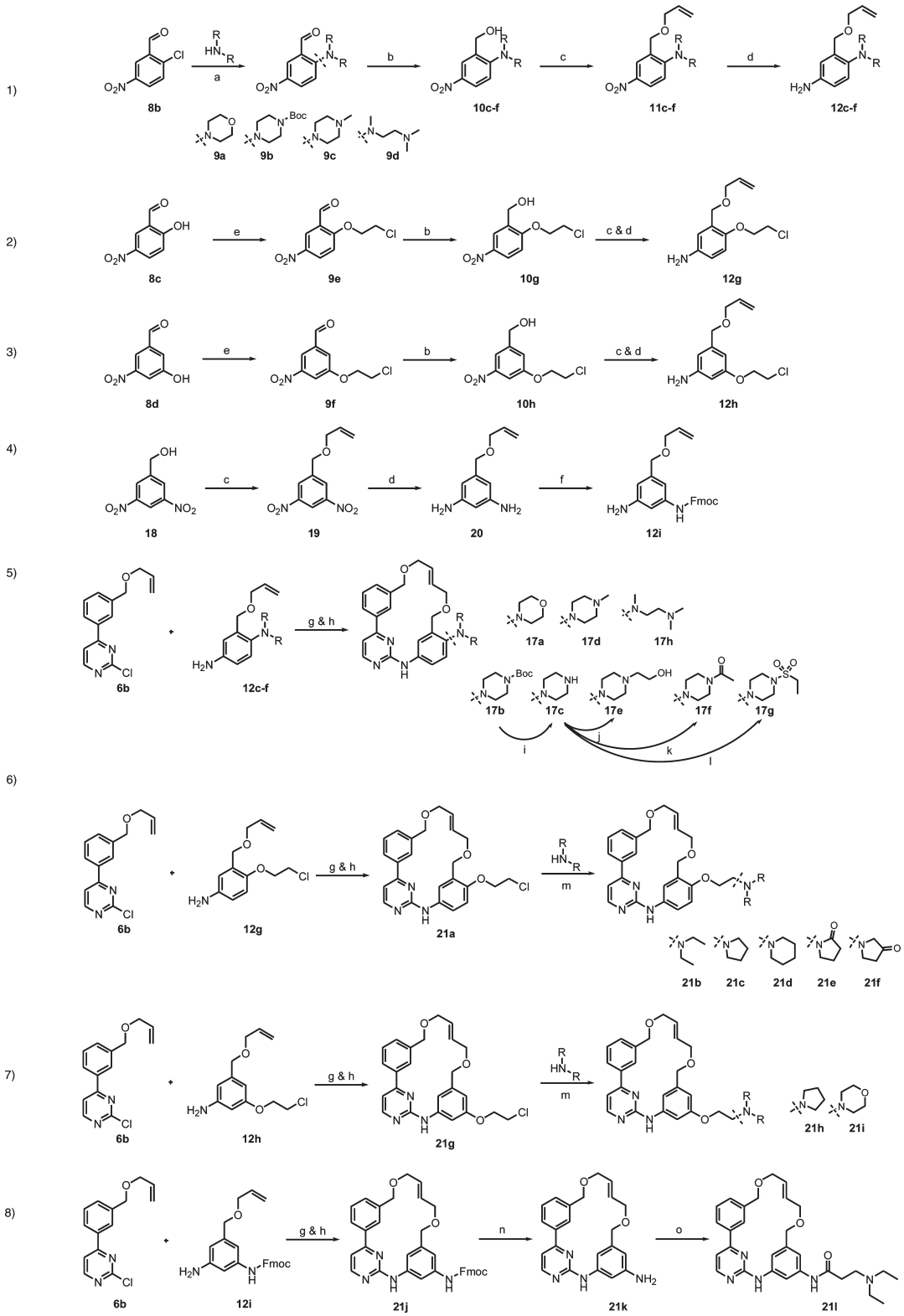

[a] Reactions and conditions: (a) K_2CO_3, DMF, 90 °C, quantitative. (b) $NaBH_4$, THF, water, 0 °C, quantitative. (c) Allyl bromide, KOH, $TBAHSO_4$, CH_2Cl_2, rt, 38−68%. (d) Fe powder, NH_4Cl, EtOH, water, 80 °C, 71−96%. (e) 1,2-Dichloroethane, K_2CO_3, DMF, 100 °C, 54−72%. (f) Fmoc-Cl, DIEA, 1,4-dioxane, rt, 95%. (g) 4 M HCl, *n*-butanol, 80−100 °C, 21−92%. (h) Either Grubbs second generation catalyst or Zhan catalyst-1B, HCl, CH_2Cl_2, 40−45 °C, 43−96%. (i) TFA, CH_2Cl_2, 40 °C, 73%. (j) 2-Bromoethanol, Et_3N, CH_2Cl_2, rt, 34%. (k) Acetyl chloride, Et_3N, CH_2Cl_2, rt, 63%. (l) Ethanesulfonyl chloride, K_2CO_3, THF, 70 °C, 41%. (m) DMA, microwave 80 °C, 72−90%. (n) 20% v/v piperidine in CH_2Cl_2, rt, 82%. (o) 3-(Diethylamino)propionic acid hydrochloride, HOBt, EDCI, CH_2Cl_2, 55%.

dx.doi.org/10.1021/jm200326p |*J. Med. Chem.* 2011, 54, 4638–4658

Scheme 3[a]

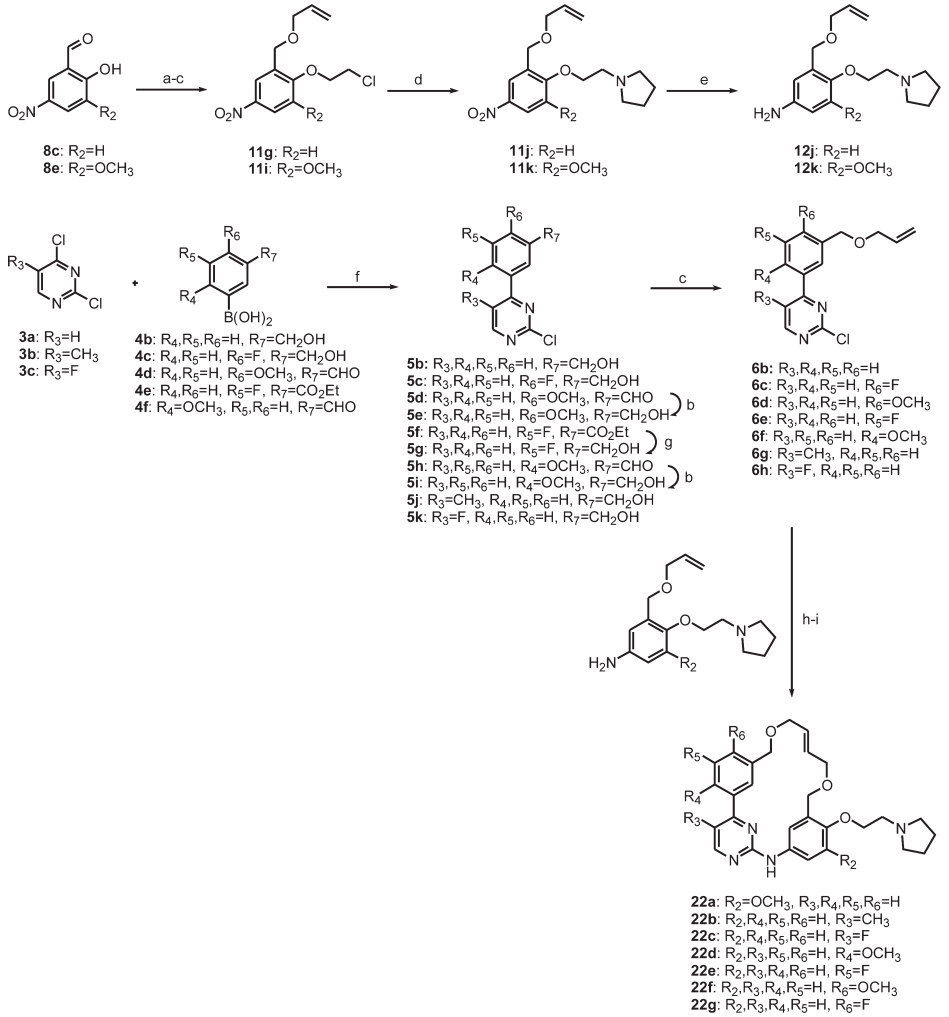

[a] Reactions and conditions: (a) 1,2-dichloroethane, K_2CO_3, DMF, 100 °C, 54−72%. (b) $NaBH_4$, THF, water, 0 °C, quantitative. (c) Allyl bromide, KOH, $TBAHSO_4$, CH_2Cl_2, rt, 38−68%. (d) Pyrrolidine, DMA, 90 °C, 66−76%. (e) Fe powder, NH_4Cl, EtOH, water, 80 °C, 74−90%. (f) $Pd(PPh_3)_4$, Na_2CO_3, 1,2-dimethoxyethane, water, 80 °C, 40−66%. (g) DIBAL, CH_2Cl_2, 0 °C, 48%. (h) 4 M HCl, *n*-butanol, 80−100 °C, 21−91%. (i) Either Grubbs second generation catalyst or Zhan catalyst-1B, HCl, CH_2Cl_2, 40−45 °C, 32−79%.

RESULTS AND DISCUSSION

Selection of the Preferred Linker. Macrocycles as protein kinase inhibitors have been explored by few other groups with no advanced candidates being reported to our knowledge. We aimed to identify a distinct core structure with clear novelty and structural rigidity which would in turn reduce conformational freedom, potentially increasing the likelihood of finding compounds with specific selectivity profiles. Hence, we decided to focus on linkers retaining the double bond conveniently installed directly from the RCM reaction. A study of various linkers with and without R1 groups demonstrated that these templates inhibited JAK2/FLT3 with selectivity against JAK1/3 and CDK2 (Table 1). In general, the most potent JAK2 linkers were 8 atoms in length with at least one benzylic ether, as in compounds **16c**, **e**, and **f**. Very good selectivity over JAK1, JAK3, and CDK2 was already apparent especially with bisphenolic ether **16a** and phenolic-benzylic ether **16c**. Symmetrical dibenzylic linkers, as employed in compounds **16e** and **16f**, were quite potent against JAK2 and retained good selectivity over JAK1 and 3 as well as CDK2. For example, **16e** has a JAK2 IC_{50} of 70 nM and is 27-, 17-, and 12-fold selective against JAK1, JAK3, and CDK2, respectively. TYK2 SAR tended to broadly track with JAK2. We decided to focus on progression of the most potent dibenzylic compounds **16e** and **16f**. At this early stage, we were already concerned about very low solubility in these high cLogP compounds (**16b** and **16d** were <10 μg/mL in PBS buffered at pH 7.0); hence, the search for locations to install a solubilizing group was paramount.

Development of More Soluble Compounds: Exploration of Substituents on the C-Ring Oriented toward Solvent. Docking of **16e** into the JAK2 ATP binding site supported the hypothesis that the expected hinge binding mode is preferred with hydrogen bonding between the amino-pyrimidine and the backbone Leu932 residue (Figure 2A). An additional hydrogen bond between the benzylic ether oxygen and Ser936 could explain the higher potency of **16c**−**f** compared to that of phenolic **16a**−**b**. Clearly, the macrocycle structure fills out the available space in the

dx.doi.org/10.1021/jm200326p | *J. Med. Chem.* 2011, 54, 4638–4658

Table 1. SAR Lead Identification: Search for a Suitable Linker for Selectivity toward JAK2

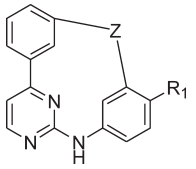

Cpd[a]	-Z-	R_1	JAK2 IC_{50} (μM)[b]	JAK1 IC_{50} (μM)[b]	JAK3 IC_{50} (μM)[b]	TYK2 IC_{50} (μM)[b]	FLT3 IC_{50} (μM)[b]	CDK2 IC_{50} (μM)[b]	cLogP
16a	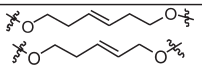	H	1.2±0.660	>10	>10	5.2±0.490	1.1±0.490	>10	4.7
16b	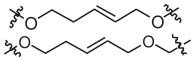	H	0.23±0.014	>10	>10	0.070±0.009	0.88±0.088	0.33±0.160	4.3
16c	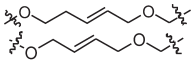	OCH_3	0.13±0.007	3.0±0.640	ND[c]	0.15±0.000	0.31±0.071	>10	4.6
16d		OCH_3	0.26±0.021	5.8±0.990	ND	0.12±0.007	0.078±0.003	0.36±0.064	4.0
16e	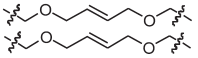	OCH_3	0.070±0.019	1.9±0.020	1.2±0.32	0.21±0.022	0.19±0.026	0.86±0.120	4.1
16f		OH	0.053±0.012	0.40±0.056	1.1±0.099	0.17±0.029	0.17±0.045	0.21±0.056	3.4

[a] All compounds were isolated as inseparable c.85:15 trans/cis mixtures. [b] All IC_{50} values are the mean ± SD (of at least two independent experiments). The assays were run at S*BIO using TG101348 as a reference: JAK1 IC_{50} = 120 nM, JAK2 IC_{50} = 7 nM, JAK3 IC_{50} = 2650 nM (published values:[9] JAK1 IC_{50} = 105 nM, JAK2 IC_{50} = 3 nM, JAK3 IC_{50} = 996 nM). [c] Not determined.

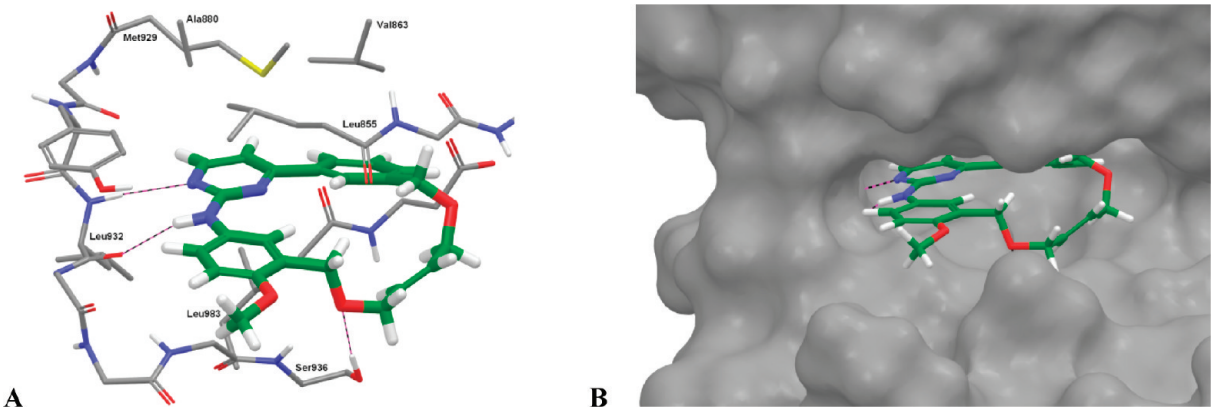

Figure 2. Compound **16e** docked into the ATP-binding site of JAK2. Compound **16e** is shown as a thick tube with green carbon. Hydrogen bonds between **16e** and JAK2 are shown as purple/black dashed lines. (A) JAK2 is shown in thin tube with gray carbon. The backbone of Leu932 forms two hydrogen bonds with **16e** and the side chain of Ser936 hydrogen bonds with an ether-oxygen in the macrocyclic linker. Leu855, Val863, Ala880, and Leu983 (in the bottom of the binding site) have hydrophobic contacts with the aromatic rings of **16e**. (B) JAK2 is shown as a surface. The methoxy group of **16e** is pointing toward a groove on the JAK2 surface that may accommodate a solubility-tag enabling fine-tuning of molecular properties.

binding site quite well but with opportunities for building additional interactions with the protein from various sites such as the pyrimidine, which we hypothesized could potentially accommodate small lipophilic groups to interact with the gatekeeper methionine residue Met929. Another possibility for additional interactions and to attach a solubilizing group is from the R1 position. Figure 2B shows that the R1 substituent points directly toward a channel out to the solvent which may offer potential for additional interactions as well as increase in solubility by installation of a basic center.

Exploration of this solvent channel from both the R1 and R2 positions proved to be quite fruitful (Table 2). A range of N- and O-substituents were very well tolerated with, on the whole, sub-100 nM IC_{50} values against the primary targets JAK2 and FLT3. Sterically large groups such as morpholine **17a** and piperazines **17c**−**d** were potent and selective, although sparingly soluble in aqueous media. Improved solubility was achieved with the polar hydroxyethyl piperazine **17e**; however, improvement in JAK2 activity seemed elusive with nitrogen-linked compounds, even with the less sterically encumbered open-chain analogues **17h** and amide **21l**. Compound **17h** is noteworthy due to its surprising CDK2 potency, likely due to a salt bridge interaction with Asp86 made possible by the methyl substitution on the nitrogen of the side-chain, which allows the side-chain to adopt an energetically favorable conformation for interaction between Asp86 and the charged dimethylamine (see Supporting Information, Figure S1). However, improved potency was achieved with oxygen-linked substituents: compounds **21b**−**f**, containing an aminoethylether side-chain, were uniformly potent against JAK2 and selective against JAK1/3 and

dx.doi.org/10.1021/jm200326p | J. Med. Chem. 2011, 54, 4638–4658

Table 2. SAR Optimization: Study of Suitable Solubilizing Groups

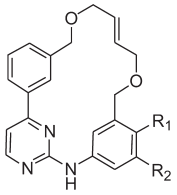

Cpd	R_1	R_2	JAK2 IC_{50} (μM)[a]	JAK1 IC_{50} (μM)[a]	JAK3 IC_{50} (μM)[a]	TYK2 IC_{50} (μM)[a]	FLT3 IC_{50} (μM)[a]	CDK2 IC_{50} (μM)[a]	cLogP	Solubility μg/ml[b]
17a	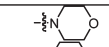	H	0.060±0.001	8.7±1.1	ND[c]	0.16±0.014	0.032±0.012	>10	4.0	ND
17c	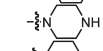	H	0.083±0.011	2.5±0.21	1.6±0.21	0.14±0.021	0.049±0.011	3.4±0.28	3.5	8.79
17d	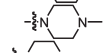	H	0.041±0.005	3.6±0.41	ND	0.19±0.026	0.030±0.007	>10	3.8	26.43
17e	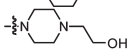	H	0.084±0.001	3.1±0.28	2.5±0.28	0.16±0.007	0.070±0.005	3.7±0.21	3.2	150
17f	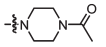	H	0.12±0.00	2.8±0.57	6±0.92	0.11±0.000	0.038±0.005	6.2±0.57	3.4	ND
17g	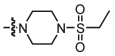	H	0.15±0.021	>10	>10	0.14±0.035	0.15±0.028	>10	3.7	ND
17h		H	0.077±0.006	3.6±0.57	ND	0.071±0.011	0.031±0.019	0.088±0.00	4.0	171
21a		H	0.22±0.035	>10	>10	0.47±0.078	0.076±0.004	>10	5.0	ND
21b	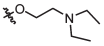	H	0.024±0.000	3.5±0.21	0.62±0.050	0.079±0.004	0.029±0.003	4.7±1.13	4.5	147
21c	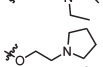	H	0.023±0.006	1.28±0.37	0.52±0.11	0.050±0.006	0.022±0.006	3.9±1.07	4.1	>150
21d	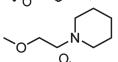	H	0.015±0.003	0.95±0.39	0.75±0.25	0.084±0.018	0.034±0.010	2.7±1.1	4.6	ND
21e	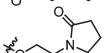	H	0.022±0.002	1.3±0.13	0.50±0.066	0.18±0.017	0.14±0.043	9.4±1.3	3.6	ND
21f	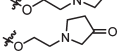	H	0.022±0.001	0.94±0.00	0.38±0.092	0.14±0.028	0.067±0.016	5.8±0.42	3.1	ND
21h	H	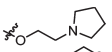	0.048±0.002	2.1±0.071	0.83±0.014	0.080±0.001	0.022±0.006	0.57±0.014	4.5	145
21i	H	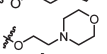	0.096±0.001	2.4±0.071	3.3±0.21	0.081±0.009	0.019±0.005	2.7±0.42	3.7	40
21k	H		0.035±0.001	ND	ND	ND	0.052±0.003	0.24±0.028	2.9	25
21l	H	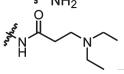	0.044±0.004	1.9±0.21	0.39±0.15	0.018±0.005	0.078±0.007	0.40±0.11	4.0	ND

[a] All IC_{50} values are the mean ± SD (of at least two independent experiments). [b] High throughput solubility in PBS buffered at pH 7.0. [c] Not determined.

CDK2 whether or not they contained a basic center. Nonbasic **21e** suffered a reduction in FLT3 as well as TYK2 activity and was likely to be less soluble than analogues with charged side chains at physiological pH; hence, the preferred compounds from this series were **21b**,**c**,**d** and **f**. The direct R2 analogue of **21c**, **21h**, was also potent against JAK2 but with submicromolar CDK2 activity. Morpholine analogue **21i**, however, was less CDK2 potent but suffered a 5-fold reduction in JAK2 potency over the most potent R_1 compounds. Nitrogen-linked anline **21k** and amide **21l** were also potent JAK2/FLT3 inhibitors but had reduced selectivity against CDK2. TYK2 SAR was in general quite flat for these compounds with the notable exception of **21l** (TYK2 IC_{50} = 18 nM). Hence, only a limited study of R_2 substituents was carried out. Aminoethylethers **21b**−**d** containing side-chains were prioritized for further evaluation in DMPK assays.

Development of More Potent Compounds: Exploration of A-Ring and B-Ring SARs. Docking of **21c** into the JAK2 ATP binding site confirmed the expected hinge binding mode between the amino-pyrimidine and the backbone Leu932 residue as well as the hydrogen bond to Ser936 from one of the oxygens in the macrocyclic linker. An additional notable interaction between the basic nitrogen of the pyrrolidine, forming a salt bridge to Asp939, could explain the improved potency against JAK2 (Figure 3A). The macrocyclic structure of **21c** with the pendant side-chain fills out the available space in the binding site with opportunities to fine-tune hydrophobic interactions with the protein from various sites of the molecule, such as the A-ring (biaryl phenyl) and B-ring (pyrimidine). From the docking analysis, we hypothesized that these two rings could potentially accommodate small lipophilic groups that could complement the hydrophobic area bound by the gatekeeper Met929, Glu930, Ala880, and Val863 (Figure 3B).

Indeed 5′-methyl substituted pyrimidine **22b** exhibited 4-fold higher potency for JAK2 (IC_{50} 6 nM) as compared to **21c** (Table 3 and Figure 4). The methyl group in the 5-position of the

dx.doi.org/10.1021/jm200326p | J. Med. Chem. 2011, 54, 4638–4658

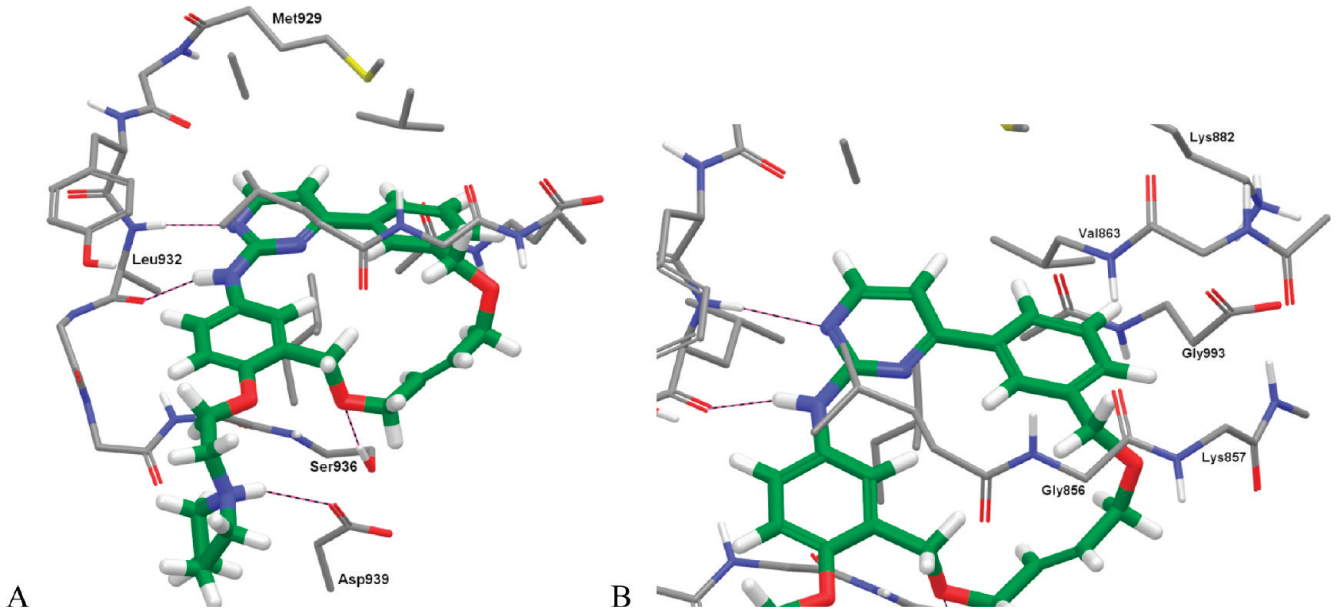

Figure 3. Compound **21c** docked into the ATP-binding site of JAK2. Compound **21c** forms the same hydrogen bonds with JAK2 as **16e**. In addition, the solubilizing pyrrolidine side-chain forms a salt bridge with Asp939. There are opportunities for hydrophobic interactions with (A) Met929 through derivatization of the 5′-pyrimidine position and (B) with Gly993/Asp994 and Lys857 accessible from the A-ring.

Table 3. SAR Exploration of Aromatic Ring Substitutions with Small Groups

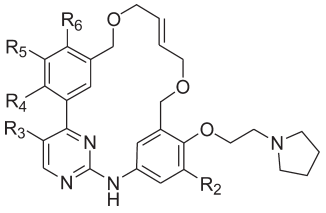

cpd	R_2	R_3	R_4	R_5	R_6	JAK2 IC_{50} (μM)[a]	JAK1 IC_{50} (μM)[a]	JAK3 IC_{50} (μM)[a]	TYK2 IC_{50} (μM)[a]	FLT3 IC_{50} (μM)[a]	CDK2 IC_{50} (μM)[a]	cLogP	solubility (μg/mL)[b]
22a	OCH_3	H	H	H	H	0.036 ± 0.003	1.7 ± 0.28	ND[c]	0.17 ± 0.021	0.006 ± 0.001	3.4 ± 1.1	4.5	154
22b	H	CH_3	H	H	H	0.007 ± 0.000	1.0 ± 0.0	0.089 ± 0.004	0.057 ± 0.004	0.019 ± 0.001	>10	4.6	178
22c	H	F	H	H	H	0.017 ± 0.000	0.83 ± 0.085	1.0 ± 0.00	0.14 ± 0.028	0.015 ± 0.003	1.55 ± 0.071	4.7	ND
22d	H	H	OCH_3	H	H	0.33 ± 0.00	4.9 ± 0.85	7.2 ± 0.21	0.62 ± 0.064	0.012 ± 0.001	>10	4.6	ND
22e	H	H	H	F	H	0.024 ± 0.002	0.38 ± 0.014	ND	0.036 ± 0.003	0.008 ± 0.004	2.0 ± 0.42	5.2	2.61
22f	H	H	H	H	OCH_3	0.019 ± 0.002	>10	0.89 ± 0.042	0.18 ± 0.00	0.092 ± 0.011	>10	4.5	60.83
22g	H	H	H	H	F	0.025 ± 0.001	4.6 ± 0.35	0.72 ± 0.11	ND	0.040 ± 0.015	3.25 ± 0.071	4.7	ND

[a] All IC_{50} values are the mean ± SD (of at least two independent experiments). [b] High throughput solubility in PBS buffered at pH 7.0. [c] Not determined.

pyrimidine fits snugly into the hydrophobic area bound by the gatekeeper Met929, Glu930, Ala880, and Val863. Although having good solubility, this compound was compromised somewhat by its selectivity against JAK3 which had dropped to about 15-fold. This may be due to the increase in torsion angle between the two aromatic rings leading to a binding conformation favorable for JAK3. Furthermore, this conformation docks less well into the CDK2 binding site with the compound fitting less well into the hydrophobic area.

Replacing the 5′-methyl group with electron-withdrawing fluoro (**22c**) reduced JAK2 activity by 3-fold, confirming that hydrophobic groups are ultimately preferred, but selectivity toward JAK1 and JAK3 was retained (Table 3). This compound was also more potent against CDK2 but retained selectivity of 91-fold. Substitution on the A ring was studied with a small group of synthetically accessible compounds. Substitution with methoxy at R_4 (**22d**) is unfavorable for JAK family activity but suggests that this area could be an avenue for the preparation of selective FLT3 inhibitors (**22d** FLT3 IC_{50} 12 nM). In contrast, substitution with electron-withdrawing fluoro at R_5 (**22e**) is well tolerated but reduces selectivity over JAK1 as well as being of very low solubility. Small lipophilic groups at the R_6 position, such as methoxy **22f**,

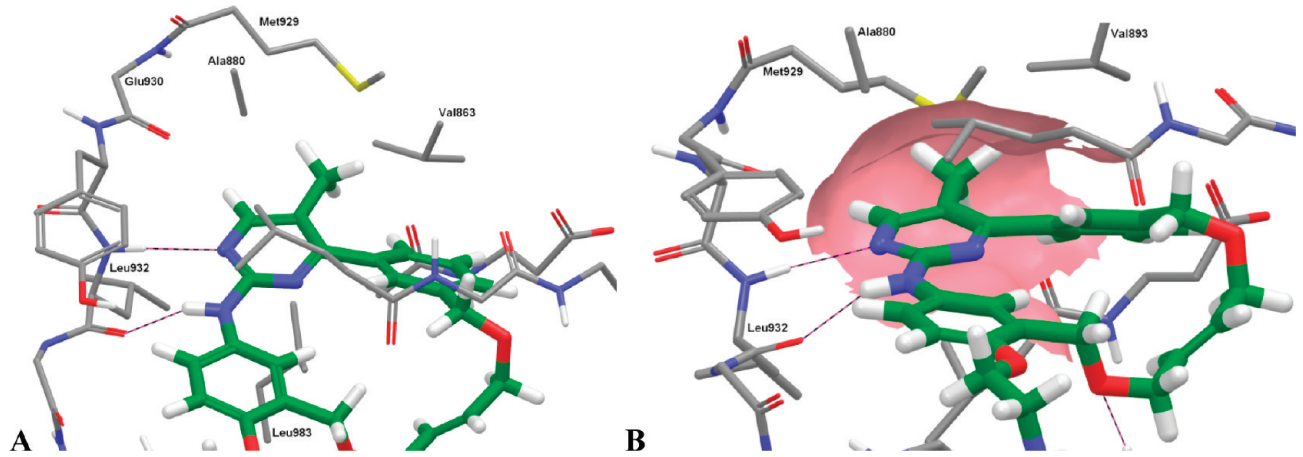

Figure 4. Compound **22b** docked into the ATP-binding site of JAK2 (A) and with the surface shown (B). The solvent-accessible surface of JAK2 surrounding the methyl-pyrimidine substituent is shown in peach. The methyl is an excellent fit to this part of the binding site.

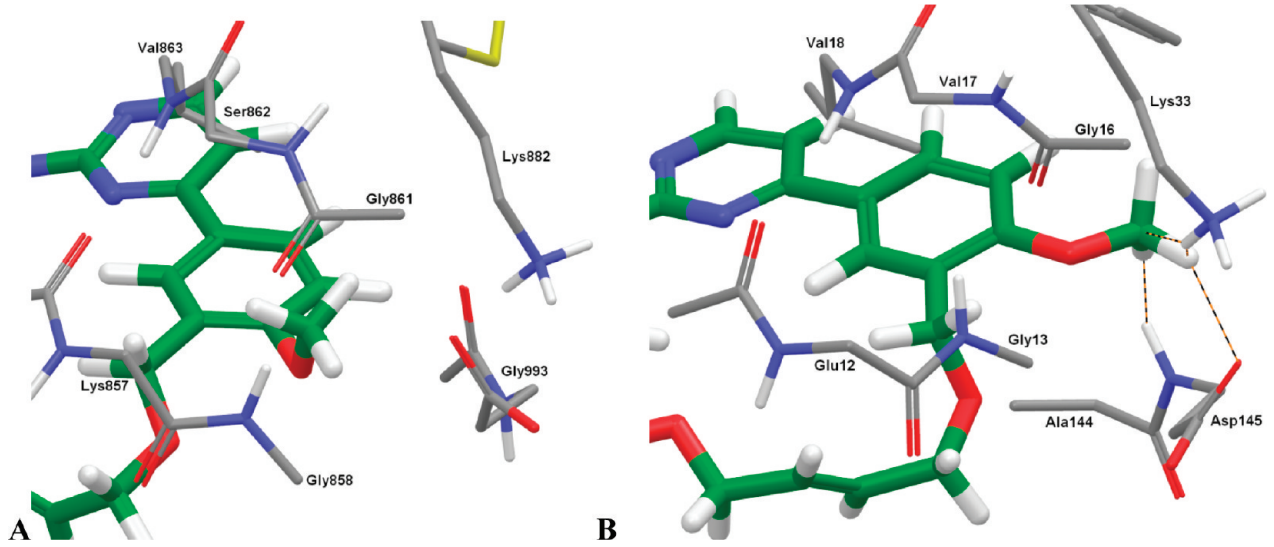

Figure 5. Compound **22f** docked into JAK2 (A) and CDK2 (B). The 4-methoxy substituent of the A-ring points up into the hydrophobic area in JAK2 while it is in the plane of the A-ring in the CDK2 pose making unfavorable contact with the charged side chains of Lys33 and Asp145.

appear to be well tolerated on this ring exhibiting excellent potency and selectivity for JAK2 over JAK1. Although the effects of adding JAK1 activity to a JAK2 inhibitor are poorly understood, we prioritized more selective compounds in the expectation that they would have reduced off-target toxicity. In general, solubility seems to be lower with substitutions on this ring, possibly as a result of high log *P*. The favorable potency and excellent selectivity of **22f** were suggested from Figure 3B and explained in Figure 5 where the extra methoxy group makes favorable hydrophobic interactions with JAK2 but has unfavorable clashes with Lys33 and Asp145 of CDK2.

Adding an additional substituent to the right-hand side aniline ring of **21c**, to give the electron rich **22a** did not compromise JAK2 activity or selectivity and showed improved FLT3 activity as compared with **21c** and, curiously, solubility. It is not apparent why there are such solubility differences within the series. Generally all compounds in this series were satisfactorily selective against CDK2 with TYK2 activity being up to 10-fold less active than JAK2.

Further in Vitro Profiling of Preferred Compounds. Compounds with JAK2 and FLT3, IC_{50} <25 nM, SI >25 for JAK1/3 and SI >100 for CDK2, were shortlisted for further celluar and in vitro ADME profiling (Table 4). Inhibition of the major metabolizing cytochrome P450 isozymes 3A4 and 2D6 were determined to identify any potential drug−drug interaction liabilities. Human and mouse liver microsomal stabilities give an indication of significant phase 1 metabolism events in target species. Physicochemical measurements assessing solubility and permeability were included as important indicators of oral absorption as well as cell penetration. Pharmacological activity in cell lines reflective of the target enzymes focused initially on cell proliferation using a Ba/F3 cell line harboring the JAK2 V617F mutation and MV4−11 cells harboring the drug resistant FLT3 D835Y mutation. Good potency in these cell lines was observed for all compounds with IC_{50} values in the range of 100−180 nM in Ba/F3 cells and 37−85 nM in MV4−11 cells. Furthermore, **21c** inhibited the JAK2-mediated production of p-STAT5 and

dx.doi.org/10.1021/jm200326p |*J. Med. Chem.* 2011, 54, 4638–4658

Table 4. In Vitro Profiling Leading to Selection of in Vivo Candidate 21c

		IC$_{50}$ Selectivity Index												
cpd	JAK2 IC$_{50}$ (μM)[a]	JAK1/ JAK2	JAK3/ JAK2	TYK2/ JAK2	CDK2/ JAK2	FLT3 IC$_{50}$ (μM)[a]	solubility (μg/mL)[b]	CYP3A4 IC$_{50}$ (μM)[a,c]	CYP2D6 IC$_{50}$ (μM)[a,c]	HLM $t_{1/2}$ (min)	MLM $t_{1/2}$ (min)	Ba/F3-JAK2 V617F GI$_{50}$ (μM)	MV4−11 GI$_{50}$ (μM)	PAMPA P_{app} (x 10^{-6} cm/s)
21b	0.024	146	26	3.3	196	0.029	147	2.8	>10	44	16	0.15	0.037	15.8
21c	0.023	56	23	2.2	170	0.022	>150	>5[d]	>5[d]	>60	22	0.16	0.047	9.3
21d	0.015	63	50	5.6	180	0.026	ND[e]	0.37	>10	>60	11	0.16	ND[e]	3.93
22b	0.007	143	13	8.1	>1000	0.019	>150	2.5	>10	>60	40	0.18	0.051	16.8
22f	0.019	>500	47	9.5	>500	0.15	60.83	>10	>10	>60	29	0.10	0.085	10.1

[a] All IC$_{50}$ values are the means (of at least two independent experiments). [b] High throughput solubility in PBS buffered at pH 7.0. [c] CYP activity determined in the human liver microsome system, see experimental section for details. [d] 20% inhibition at 5 μM. [e] Not determined.

Table 5. Physico-Chemical Properties and in Vitro ADME of 21c

property	value
mol. wt.	472.58
no. of HBD	1
no. of HBA	6
cLogP	4.1
PSA (Å^2)	69
HLM ($t_{1/2}$, min)	>60
DLM ($t_{1/2}$, min)	41
RLM ($t_{1/2}$, min)	18
MLM ($t_{1/2}$, min)	22
human CYP inhibition IC$_{50}$ (μM)[a]	>5[b]
permeability ($P_{app,\ A\rightarrow B}$, $\times 10^{-6}$ cm/s)[c]	16
plasma protein binding (%)[d] in human	99.88
plasma protein binding (%) in dog	99.63
plasma protein binding (%) in mouse	99.41

[a] Human CYP3A4, 1A2, 2D6, 2C9, 2C19. [b] Precipitation observed at highest concentration of 25 μM. No significant inhibition observed at 5 μM. [c] Caco-2 bidirectional permeability assay. [d] Equilibrium dialysis assay in human plasma at 1000 ng/mL.

Table 6. Oral Pharmacokinetic Parameters of 21c in Mice, Rats, and Dogs[a]

parameter	mouse[b] (n = 3/time point)	rat[c] (n = 3)	dog[c] (n = 4)
dose (mg/kg)	30	10	3
C_{max} (ng/mL)	292	114 ± 25	11.5 ± 11.8
t_{max} (h)	1.0	4 ± 0	2.0[d]
$t_{1/2}$ (h)	0.84	5.7 ± 1.3	3.4 ± 0.8
AUC$_{0\text{-}t}$ (ng·h/mL)[e]	399	599 ± 111	53 ± 53

[a] Note: In preliminary PK screening studies, **21c** showed oral bioavailability of 39%, 24%, and 10% in mice, dogs, and rats, respectively. [b] Mean. [c] Mean ± SD. [d] Median. [e] t = 8 h.

p-STAT3 dose dependently in Ba/F3 cells, and the production of p-FLT3 and p-STAT5 in MV4−11 cells (see Supporting Information, Figures S2 ansd S3). This evidence of intracellular target inhibition was further supported by high permeability and solubility. Differences in metabolic parameters were more apparent between compounds: CYP 3A4 was a particular area of differentiation where **22b**, although exhibiting desirable single digit nanomolar potency toward JAK2, had an IC$_{50}$ of 2.5 μM for CYP3A4. Although stable in liver mircosomes, **22b** had lower selectivity for JAK3. CYP3A4 inhibition was clearly an undesirable feature of piperidine analogue **21d**, reducing our interest in further studies with this compound. Diethylamine analogue **21b** suffered from low stability in mouse and moderate stability in human microsomes in addition to significant CYP3A4 inhibition. Although the CYP inhibition for **21b** and **22b** was moderate, it could not be excluded as these plasma concentrations could be reached in human subjects, and the compounds were therefore not further tested. However, **21c** and **22f** were much less active against CYP3A4 (20% inhibition at 5 μM and IC$_{50}$ >10 μM, respectively), and both compounds had good selectivity and microsomal stability. Compound **22f**, although possessing excellent enzyme selectivity, was less active against FLT3. Methyl pyrimidine **22b** and **21c** are differentiated by a single methyl group which generates subtle, but important, differences in the compound profiles. Compound **21c** exhibits an overall balanced profile meeting all target criteria. It was also shown to be active against the V617F mutant of JAK2 with IC$_{50}$ = 19 nM and the D835Y mutant of FLT3 with IC$_{50}$ = 6 nM, and its protein kinase selectivity was confirmed by testing against more than 50 other protein kinases covering all major families of the human protein kinome.[19]

Thus, **21c** was selected for further profiling (Table 5). Preferred properties for an orally administered drug are all exhibited by **21c**: molecular weight <500, number of hydrogen bond donors <5 and acceptors <10, and cLogP <5 and polar surface area <120 Å^2. None of the five major drug metabolizing human CYP450s (1A, 3A4, 2D6, 2C9, and 2C19) is inhibited by **21c** implying low drug−drug interaction potential. A Caco-2 bidirectional permeability assay confirmed that **21c** has high permeability and was not a substrate for *P*-glycoprotein (efflux ratio of 0.8), hence predicting high intestinal absorption. In vitro plasma protein binding to human plasma was high (99.9%), but taken together, the in vitro ADME profile of **21c** supports daily oral dosing.

Pharmacokinetics of 21c in Multiple Species. The PK properties of **21c** are summarized in Table 6. Compound **21c** showed rapid absorption in mice (t_{max} =1.0 h), a mean C_{max} and AUC of 292 ng/mL and 399 ng·h/mL, respectively, with a mean terminal half-life of 0.8 h following a single oral dose of 30 mg/kg. The promising efficacy of **21c** in several preclinical pharmacology models (see below) was consistent with this exposure. In rats, **21c** showed moderately fast absorption (t_{max} = 4 h), with a peak concentration of 114 ng/mL, AUC of 599 ng·h/mL, and a terminal half-life of ~6 h following a single oral dose of 10 mg/kg. In

dx.doi.org/10.1021/jm200326p | J. Med. Chem. 2011, 54, 4638–4658

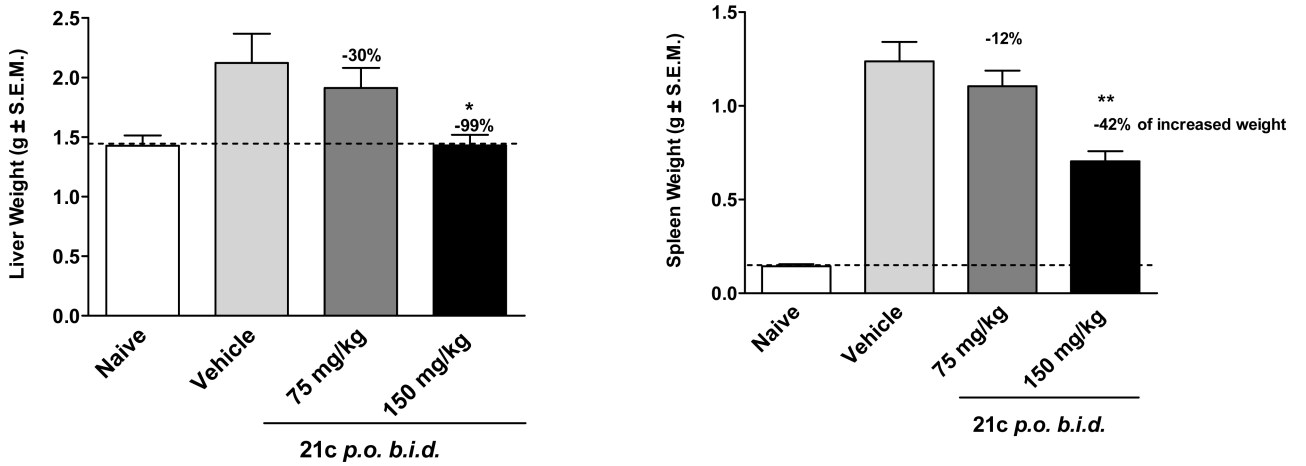

Figure 6. Compound **21c** reduces splenomegaly and hepatomegaly in a Ba/F3-JAK2^{V617F} model of leukemia. Ba/F3-JAK2^{V617F}-bearing nude mice were dosed p.o., b.i.d., with 75 and 150 mg/kg **21c** (HCl salt) for 13 consecutive days. On day 13, mice were sacrificed and spleen and liver weights determined (n = 8; * p < 0.05, **p < 0.01 ANOVA, Dunnett's post test). The dotted line represents baseline weights.

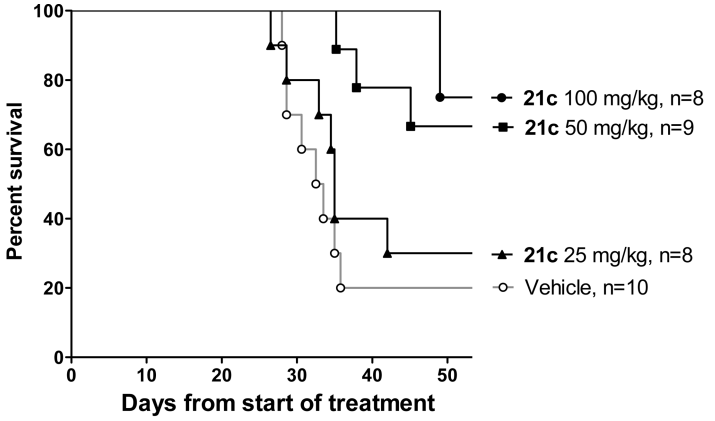

Group A Group B	Vehicle 21c (25 mg/kg)	Vehicle 21c (50 mg/kg)	Vehicle 21c (100 mg/kg)
Chi square	0.6210	6.848	7.819
df	1	1	1
P value	0.4307	0.0089	0.0052
P value summary	ns	**	**
Are the survival curves significantly different?	No	Yes	Yes
Median survival			
Group A	33.00	33.00	33.00
Group B	35.00	55.00	55.00
Ratio	0.9429	0.6	0.6
95% CI of ratio	0.5266 to 1.359	0.1937 to 1.006	0.2053 to 0.9947
Hazard Ratio			
Ratio	1.534	5.479	6.735
95% CI of ratio	0.5293 to 4.445	1.533 to 19.58	1.769 to 25.64

Figure 7. Compound **21c** is efficacious in a xenograft derived from a cell line harboring FLT3-ITD. MV4−11 tumor bearing nude mice were randomized into 4 groups of 8−10 animals each. Mice were treated orally (p.o.) once daily at doses of 25, 50, or 100 mg/kg of **21c** for 21 consecutive days, and median time to end point (= median survival) was determined on day 55. The figures given indicate doses calculated using the molecular weight of the free base. The Log-rank (Mantel-Cox) test was used for statistical analysis.

dogs, **21c** was rapidly absorbed (t_{max} = 2.0 h), with a peak concentration of ~12 ng/mL, AUC of 53 ng·h/mL, and a terminal half-life of 3.4 h following a single oral dose of 3 mg/kg.

Efficacy of 21c in Mouse Models. On the basis of its efficacy on JAK2 and FLT3 dependent tumor cell lines[19] and good oral bioavailability, **21c** was selected for evaluation in mouse tumor

models. Two models were selected on the basis of their relevance to the molecular targets: Ba/F3-JAK2^{V617F} and MV4−11 allograft and xenograft studies representing cell lines dependent on mutant JAK2 and FLT3 signaling, respectively.

The Ba/F3-JAK2^{V617F} mouse allograft represents a model for a JAK2-driven disease exhibiting hallmark symptoms of myeloproliferative diseases such as splenomegaly and hepatomegaly. In this model, murine Ba/F3-JAK2^{V617F} cells were engrafted by tail vein injection. Treatment with **21c** at doses of 75 and 150 mg/kg p.o. b.i.d. was started 4 days after cell inoculation for 13 consecutive days. At study termination, vehicle control mice exhibited splenomegaly and hepatomegaly (∼7-fold and 1.6-fold respectively); **21c** treatment at 150 mg/kg p.o. b.i.d. significantly ameliorated the disease symptoms, with 42% normalization of spleen weight and 99% normalization of liver weight (Figure 6).

For evaluation of the in vivo efficacy of **21c** on FLT3-ITD driven tumors, MV4−11 xenografts were established in nude mice. To identify effects on tumor growth delay, MV4−11 tumor bearing mice (average starting tumor size of 130 mm^3) were treated orally once daily at doses of 25, 50, or 100 mg/kg for 21 consecutive days. After termination of the treatment, tumor growth was measured up to day 55, and median time-to-end point (= median survival) was calculated. The end point of the experiment for an individual mouse was reached on day 55 or when the tumor reached a size of 1000 mm^3, whichever occurred earlier. Figure 7 shows the Kaplan−Meier survival curves for the different groups. The median survival was 33.0 days for the vehicle group. The lowest dose-treated group (25 mg/kg **21c**) did not show statistically significant activity with survival of 35.0 days. However, the 50 mg/kg and 100 mg/kg **21c** treatment groups showed a significantly increased median survival of 55 days ($p < 0.01$) with no significant body weight loss in the treated animals at the termination of the study. Clearly, **21c** is effective at lower doses in the MV4−11 model than in the more aggressive Ba/F3 JAK2^{V617F} model. This is partly explained by differences in the degree of oncogene addiction in the two models, reflected in the cell viability IC_{50} of both cell lines: the MV4−11 cell line is more sensitive than the Ba/F3 JAK2^{V617F} cell line (MV4−11 showed an approximately 4-fold difference in sensitivity compared to that of Ba/F3 JAK2^{V617F}); this may account for the difference in dose required in vivo. Both 75 mg/kg and 150 mg/kg bid doses are well tolerated in the Ba/F3 inoculated animals with no significant body weight loss.

CONCLUSIONS

We have described the discovery of a series of small molecule macrocycles as potent inhibitors of JAK2 and FLT3 kinases. SAR studies using data from biochemical and ADME assays led to potent JAK2 inhibitors with an appropriate balance of physicochemical and ADME properties suitable for daily oral dosing. Our original hypothesis of using a macrocyclic structure with limited conformational options by constraining the binding moieties at specific points in space has produced a novel series of JAK2/FLT3 selective inhibitors able to achieve interactions in the active sites of the target enzymes not easily accomplished with an acyclic structure. A subset of diverse compounds showed good potency and selectivity for JAK2 within the JAK family, good potency for FLT3, and also retaining potency for TYK2. Importantly, selectivity for CDK2 was assured in this series, which is not the case with at least one reported clinical-stage JAK1/2 inhibitor.[47] Cell proliferation was potently inhibited in cell lines driven by mutant JAK2 and FLT3, and target inhibition in the cell has been demonstrated. The favorable oral pharmacokinetic properties of **21c** prompted us to explore its pharmacodynamic effects in relevant mouse models in a dose-dependent manner. An efficacy study in a model of JAK2^{V617F}-driven disease demonstrated dose-dependent tumor growth inhibition[19] and normalization of splenomegaly and hepatomegaly at well-tolerated doses. In a second study in a model of FLT3-ITD driven leukemia, **21c** demonstrated significant survival benefits at very well-tolerated doses. Extensive cellular profiling of **21c** on myeloid and lymphoid cells and its activity in the JAK2^{V617F}-driven SET-2 model have been reported elsewhere.[19] Its attractive preclinical profile led to the selection of **21c** for preclinical development, which in turn resulted in progression into the clinic where it has shown clinical benefit in myelofibrosis[13,14] and lymphoma patients in two completed phase 2 trials.[48]

EXPERIMENTAL SECTION

Chemistry. Workup for chemical reactions was typically done by diluting the reaction mixture or residue with the reaction solvent or extraction solvent and then washing with the indicated aqueous solution(s). Product solutions were dried over anhydrous sodium sulfate prior to filtration, and the solvents were removed under reduced pressure using a rotary evaporator. All compounds were purified by either flash or reversed phase chromatography. Flash column chromatography was conducted using Silica gel 60 (Merck KGaA, 0.040−0.063 mm, 230−400 mesh ASTM). Reverse-phase preparative high performance liquid chromatography (rpHPLC) was operated on a Phenomenex column (Luna 5 μm C18 (2) 100A 150 × 21.2 mm) with adjustable solvent gradients, usually 5 to 95% acetonitrile in water + 0.1% trifluoroacetic acid (TFA), with a run time of 18 min, at a flow rate of 20 mL/min were used for routine purification. Fractions containing the desired product were lyophilized or evaporated to dryness under vacuum to provide the dry compound, or evaporated to remove volatile organic solvents, then extracted with a suitable organic solvent (ethyl acetate or dichloromethane were commonly used; if necessary, the pH of the aqueous solution was adjusted in order to get free base, acid, or the neutral compound).

The preliminary purity and identity of all compounds was assessed post-purification by tandem HPLC/mass spectral (LC/MS) analyses on a Waters Micromass ZQ mass spectrometer in electrospray ionization (ESI) positive mode after separation on Waters 2795 Separations Module. The HPLC separations were performed on a Phenomenex column (Luna 5 μm C18 (2) 100A 50 × 2.00 mm) with a flow rate of 0.8 mL/min and a 4 min gradient of x−100% acetonitrile in water + 0.05% TFA (x = 5, or 30, or 50), using a Waters 2996 photodiode array detector. Purity and identity were assessed on the integrated UV chromatogram (220−400 nm) and the mass spectrum (homogeneity of the product peak and its fragmentation(s)). The final purity was determined using Waters 2695 Separations Module on a Waters Xterra RP18 3.5 mm 4.6 × 20 mm IS column with a flow rate of 2.0 mL/min, gradient 5−65% B over 4 min, then 65−95% B over 1 min, and 95% B for an additional 0.1 min (solvent A, H_2O with 0.1% TFA; solvent B, acetonitrile with 0.1% TFA), and a Waters 2996 photodiode array detector. For compounds not suitable for the above HPLC methods either due to polarity or poor peak separation, a longer column (Phenomenex Gemini 5 μm C18, 110A, 4.6 × 150 mm) together with a flow rate of 1.0−1.2 mL/min and a 15 min gradient of 5−95% acetonitrile in water + 0.1% TFA was used for purity determination. Purity was >95% for all test compounds except those indicated in their respective synthesis descriptions.

All the 1D and 2D NMR experiments for ^{1}H (400.13 MHz), ^{13}C (100.61 MHz), ^{15}N (40.55 MHz), and ^{19}F (376.47 MHz) nuclei were performed on a Bruker AVANCE-400 digital NMR spectrometer. $^{1}H-^{1}H$, $^{1}H-^{13}C$, and $^{1}H-^{15}N$ 2D experiments (COSY, HMQC, HSQC, and HMBC) were run with Z-gradient selection. NMR spectra are reported in ppm with reference to an internal tetramethylsilane standard (0.00 ppm for ^{1}H and ^{13}C) or solvent peak(s) of $CDCl_3$ (7.26 and 77.1 ppm) or CD_3OD (3.31 and 49.0 ppm), or DMSO-d_6 (2.50 and 39.5 ppm). Other NMR solvents were used as needed. When peak multiplicities are reported, the following abbreviations are used: s = singlet, d = doublet, t = triplet, q = quartet, m = multiplet, br = broadened, dd = doublet of doublets, dt = doublet of triplets, and bs = broadened singlet. Coupling constants, when given, are reported in Hertz.

All melting points are uncorrected. Elemental analyses of CHN were performed on Perkin-Elmer 2400 CHN/CHNS Elemental Analyzers. HRMS was obtained from a Bruker microTOF-Q II with direct injection.

*3-(2-Chloro-pyrimidin-4-yl)-phenol (**5a**).* To a degassed (nitrogen) solution of 2,4-dichoropyrimidine (**3a**) (1.0 g, 6.71 mmol) and 3-hydroxylphenyl boronic acid (**4a**) (1.1 g, 8.05 mmol) in 1,2 dimethoxyethane (10 mL) was sequentially added aqueous Na_2CO_3 (1.06 g, 10.06 mmol) and $Pd(PPh_3)_4$ (0.387 g, 0.335 mmol). The resultant mixture was stirred at 80−85 °C for 4 h, cooled to 0 °C, and quenched with saturated NH_4Cl. The product was extracted with CH_2Cl_2 thrice and the combined organic extracts were washed with brine, dried over Na_2SO_4, and concentrated under reduced pressure. The crude mixture was column purified (EtOAc/Hexane) to furnish 0.550 g of **5a** (yield, 40%). LC-MS (ESI positive mode) m/z 207 ($[M + H]^+$). ^{1}H NMR (400 MHz, $CDCl_3$): δ 9.74 (s, 1H), 9.23 (d, 1H), 8.83 (d, 1H), 8.01 (dd, 1H), 7.60−7.65 (m, 1H), 7.35 (t, 1H), 6.94−6.99 (m, 1H).

*[3-(2-Chloro pyrimidine-4-yl) phenyl] Methanol (**5b**).* The synthesis for this intermediate has been improved for scale-up and was prepared using a different Suzuki coupling procedure as compared to that of **5a**. To a degassed (nitrogen) solution of **3a** (50 g, 335 mmol) and 3-(hydroxymethyl)phenylboronic acid (**4b**) (48.5 g, 318 mmol) in THF (500 mL, 10 vol) was added saturated Na_2CO_3 (88.6 g, 838 mmol), palladium acetate (0.15 g, 0.67 mmol), and triphenylphosphine (0.35 g, 1.34 mmol). The resultant mixture was stirred at 70 °C for 6 h, and filtered. Water was added to the filtrate and extracted with ethyl acetate (3 × 250 mL). The combined organic extracts were washed with brine, dried (Na_2SO_4), and filtered. The filtrate was treated with activated charcoal, and the mixture was filtered and the filtrate concentrated under reduced pressure, and the crude product was slurried in isopropyl alcohol (300 mL). The mixture was filtered, and the solid was slurried in cold *n*-heptane and filtered to furnish **5b** (42.8 g; yield, 61%). This material was taken up for the next step without any purification. LC-MS (ESI positive mode) m/z 221 ($[M + H]^+$); ^{1}H NMR (DMSO-d_6) δ 8.81 (d, 1H), 8.15 (br, 1H), 8.10 (d, 1H), 8.04 (dt, 1H), 7.57−7.54 (m, 1H), 4.63 (s, 2H); ^{13}C NMR (DMSO-d_6) δ 166.7, 161.4, 160.8, 143.9, 134.7, 130.5, 129.4, 126.1, 125.4, 116.4, 62.9.

Following a procedure similar to that of **5a**, the following intermediates were synthesized:

*[5-(2-Chloro-pyrimidin-4-yl)-2-fluoro-phenyl]-methanol (**5c**).* The title compound was synthesized from **3a** and [4-fluoro-3-(hydroxymethyl)phenyl] boronic acid (**4c**) (yield, 66%). LC-MS (ESI positive mode) m/z 239 ($[M + H]^+$).

*5-(2-Chloro-pyrimidin-4-yl)-2-methoxy-benzaldehyde (**5d**).* The title compound was synthesized from **3a** and 3-formyl-4-methoxyphenylboronic acid (**4d**) (yield, 58%). LC-MS (ESI positive mode) m/z 249 ($[M + H]^+$).

*3-(2-Chloro-pyrimidin-4-yl)-5-fluoro-benzoic Acid Ethyl Ester (**5f**).* The title compound was synthesized from **3a** and (3-fluoro-5-ethoxycarbonylphenyl) boronic acid (**4e**) (yield, 89%). LC-MS (ESI positive mode) m/z 281 ($[M + H]^+$).

*3-(2-Chloro-pyrimidin-4-yl)-4-methoxy-benzaldehyde (**5h**).* The title compound was synthesized from **3a** and 5-formyl-2-methoxyphenyl boronic acid (**4f**) (yield, 84%). LC-MS (ESI positive mode) m/z 249 ($[M + H]^+$).

*[3-(2-Chloro-5-methyl-pyrimidin-4-yl)-phenyl]-methanol (**5j**).* The title compound was synthesized from 2,4-dichloro-5-methylpyrimidine (**3b**) and **4b** (yield, 56%). LC-MS (ESI positive mode) m/z 235 ($[M + H]^+$).

*[3-(2-Chloro-5-fluoro-pyrimidin-4-yl)-phenyl]-methanol (**5k**).* The title compound was synthesized from 2,4-dichloro-5-fluoropyrimidine (**3c**) and **4b** (yield, 74%). LC-MS (ESI positive mode) m/z 239 ($[M + H]^+$).

*[5-(2-Chloro-pyrimidin-4-yl)-2-methoxy-phenyl]-methanol (**5e**).* To a solution of **5d** (5 g, 20.1 mmol) in THF (25 mL, 5 vol) at 0 °C was added $NaBH_4$ (0.76 g, 20.1 mmol), and the resulting mixture was stirred for 30 min before warming to rt. The reaction mixture was quenched with water. The product was extracted with CH_2Cl_2 thrice, and the combined organic extracts were washed with H_2O followed by brine, dried over Na_2SO_4, and concentrated under reduced pressure to furnish without purification 5 g of compound **5e** (yield, quantitative). LC-MS (ESI positive mode) m/z 251 ($[M + H]^+$).

*[3-(2-Chloro-pyrimidin-4-yl)-5-fluoro-phenyl]-methanol (**5g**).* To a cooled mixture of **5f** (560 mg, 2.0 mmol) in CH_2Cl_2 (6 mL, 10 vol) at 0 °C, 1.0 M DIBAL solution (4 mL, 4.00 mmol) was added dropwise. The resulting mixture was stirred for 1 h and allowed to warm to rt. Water was added, and the product was extracted with CH_2Cl_2 (3 × 10 mL). The combined organic extracts were washed with brine, dried (Na_2SO_4), and concentrated under reduced pressure to obtain the crude residue, which was purified by column chromatography (using 35% ethyl acetate in hexane) to furnish **5g** (230 mg; yield, 48%) as a colorless oil. LC-MS (ESI positive mode) m/z 239 ($[M + H]^+$).

*[3-(2-Chloro-pyrimidin-4-yl)-4-methoxy-phenyl]-methanol (**5i**).* The title compound was synthesized following a procedure similar to that of **5e**, from **5h** (yield, quantitative). LC-MS (ESI positive mode) m/z 251 ($[M + H]^+$).

*4-(3-Allyloxymethyl phenyl)-2-chloro Pyrimidine (**6b**).* A mixture of **5b** (20 g, 90.6 mmol), KOH (23.8 g, 172 mmol), and tetrabutyl ammonium hydrogen sulfate (1.5 g, 4.53 mmol) in allyl bromide (80 mL, 4 vol) was stirred at rt for 12 h. The reaction mixture was quenched with water and extracted with CH_2Cl_2 (3 × 25 mL). The combined organic extracts were washed with water, brine, dried (Na_2SO_4), and concentrated under reduced pressure to obtain the crude residue, which was purified by column chromatography (using 15% ethyl acetate in hexane) to furnish **6b** (13 g; yield, 55%) as a pale yellow oil. LC-MS (ESI positive mode) m/z 261 ($[M + H]^+$); ^{1}H NMR ($CDCl_3$) δ 8.62 (d, 1H), 8.06 (br, 1H), 8.00 (dt, 1H), 7.66 (d, 1H), 7.54−7.46 (m, 2H), 6.02−5.93 (m, 1H), 5.27 (ddq, 2H), 4.60 (s, 2H), 4.08 (dq, 2H); ^{13}C NMR ($CDCl_3$) δ 167.1, 161.9, 159.9, 139.7, 135.3, 134.6, 131.2, 129.7, 129.3, 126.6, 117.5, 115.4, 71.7, 71.6; IR (KBr pellet): 1568, 1535, 1344, 1186, 1079 cm^{-1}.

Following a procedure similar to that of **6b**, the following intermediates were synthesized:

*4-(3-Allyloxy-phenyl)-2-chloro-pyrimidine (**6a**).* The title compound was synthesized from **5a** and allyl bromide (yield, 59%). LC-MS (ESI positive mode) m/z 247 ($[M + H]^+$).

*4-(3-Allyloxymethyl-4-fluoro-phenyl)-2-chloro-pyrimidine (**6c**).* The title compound was synthesized from **5c** and allyl bromide (yield, 63%). LC-MS (ESI positive mode) m/z 279 ($[M + H]^+$).

*4-(3-Allyloxymethyl-4-methoxy-phenyl)-2-chloro-pyrimidine (**6d**).* The title compound was synthesized from **5e** and allyl bromide (yield, 51%). LC-MS (ESI positive mode) m/z 291 ($[M + H]^+$).

*4-(3-Allyloxymethyl-5-fluoro-phenyl)-2-chloro-pyrimidine (**6e**).* The title compound was synthesized from **5g** and allyl bromide (yield, 71%). LC-MS (ESI positive mode) m/z 279 ($[M + H]^+$).

4-(5-Allyloxymethyl-2-methoxy-phenyl)-2-chloro-pyrimidine (**6f**). The title compound was synthesized from **5i** and allyl bromide (yield, 55%). LC-MS (ESI positive mode) m/z 291 ($[M + H]^+$).

4-(3-Allyloxymethyl-phenyl)-2-chloro-5-methyl-pyrimidine (**6g**). The title compound was synthesized from **5j** and allyl bromide (yield, 42%). LC-MS (ESI positive mode) m/z 275 ($[M + H]^+$).

4-(3-Allyloxymethyl-phenyl)-2-chloro-5-fluoro-pyrimidine (**6h**). The title compound was synthesized from **5k** and allyl bromide (yield, 67%). LC-MS (ESI positive mode) m/z 279 ($[M + H]^+$).

4-(3-But-3-enyloxy-phenyl)-2-chloro-pyrimidine (**7**). To a mixture of **5a** (2.0 g, 9.68 mmol) and 4-bromo-but-1-ene (7.8 g, 5.80 mmol) in dry DMF (10 mL) at ambient temperature was added cesium carbonate (14.19 g, 43.55 mmol), and the resulting mixture was stirred at 40 °C for 6 h. The reaction mixture was cooled to 0 °C and quenched with water. The product was extracted with CH_2Cl_2 thrice, and the combined organic extracts were washed with water followed by brine, dried over Na_2SO_4, and concentrated under reduced pressure to furnish an oil, which was purified by column (EtOAc/hexane) to obtain 1.61 g of **7** (yield, 64%). LC-MS (ESI positive mode) m/z 261 ($[M + H]^+$); ^{1}H NMR (400 MHz, DMSO-d_6): δ 8.82 (d, 1H), 8.12 (d, 1H), 7.77 (d, 1H), 7.70 (br s, 1H), 7.48 (t, 1H), 7.18 (dd, 1H), 5.86−5.98 (m, 1H), 5.16−5.24 (m, 1H), 5.09−5.13 (m, 1H), 4.13 (t, 2H), 2.49−2.56 (m, 2H).

2-(4-Methyl-piperazin-1-yl)-5-nitro-benzaldehyde (**9c**). To a mixture of 2-chloro-5-nitrobenzaldehyde **8b** (3 g, 16.2 mmol) and 1-methylpiperazine (3.5 mL, 31.6 mmol) in DMF (30 mL, 10 vol) was added K_2CO_3 (4 g, 28.9 mmol), and the resulting mixture was stirred at 90 °C for 4 h. The reaction mixture was cooled to rt, and water (60 mL) was added to quench. The aqueous layer was extracted thrice with EtOAc (40 mL each), and the combined organic extract was washed with brine, dried (Na_2SO_4), and concentrated under reduced pressure. Product **9c** (3.6 g; yield, 90%) was taken forward for the next step without any purification. LC-MS (ESI positive mode) m/z 250 ($[M + H]^+$). ^{1}H NMR ($CDCl_3$): δ 10.10 (s, 1H), 8.62 (d, 1H), 8.30 (dd, 1H), 7.09 (d, 1H), 3.35−3.32 (m, 4H), 2.64−2.63 (m, 4H), 2.39 (s, 3H).

Following a procedure similar to that of **9c**, the following intermediates were synthesized:

2-Morpholin-4-yl-5-nitro-benzaldehyde (**9a**). The title compound was synthesized from **8b** and morpholine (yield, quantitative). LC-MS (ESI positive mode) m/z 237 ($[M + H]^+$).

4-(2-Formyl-4-nitro-phenyl)-piperazine-1-carboxylic Acid tert-Butyl Ester (**9b**). The title compound was synthesized from **8b** and 1-Boc-piperazine (yield, quantitative). LC-MS (ESI positive mode) m/z 336 ($[M + H]^+$).

2-[(2-Dimethylamino-ethyl)-methyl-amino]-5-nitro-benzaldehyde (**9d**). The title compound was synthesized from **8b** and *N,N,N′*-trimethyl-ethane-1,2-diamine (yield, 96%). LC-MS (ESI positive mode) m/z 252 ($[M + H]^+$).

2-(2-Chloro ethoxy)-5-nitro-benzaldehyde (**9e**). To a mixture of 2-hydroxy-4-nitrobenzaldehyde (**8c**) (50 g, 299 mmol) and 1,2-dichloroethane (300 mL, 6 vol) in DMF (600 mL, 12 vol)) was added K_2CO_3 (62.5 g, 450 mmol), and the resulting mixture was stirred at 100−105 °C for 6 h. The reaction mixture was quenched with water (500 mL), and the product was extracted four times with CH_2Cl_2 (200 mL each). The combined organic extracts were washed with water (500 mL), brine, dried (Na_2SO_4), and concentrated under reduced pressure, and *n*-hexane (500 mL) was added to the crude product. The resulting mixture was stirred for 30 min and evaporated to dryness under reduced pressure, and one more hexane washing was repeated. A third aliquot of cold *n*-hexane (500 mL) was added, and the yellow solid was collected by filtration and washing with cold *n*-hexane. Product **9e** (49.3 g; yield, 72%) was taken forward for the next step without any purification. LC-MS (ESI positive mode) m/z 230 ($[M + H]^+$); ^{1}H NMR ($CDCl_3$) δ 10.52 (s, 1H), 8.71 (d, 1H), 8.45 (dd, 1H), 7.14 (d, 1H), 4.51 (t, 2H), 3.96 (t, 2H); ^{13}C NMR ($CDCl_3$) δ 187.3, 164.2, 142.1, 130.6, 125.0, 124.6, 113.2, 69.4, 41.3.

Following a procedure similar to that of **9e**, the following intermediates were synthesized:

3-(2-Chloro-ethoxy)-5-nitro-benzaldehyde (**9f**). The title compound was synthesized from 3-hydroxy-5-nitrobenzaldehyde (**8d**) and 1,2-dichloroethane (yield, 66%). LC-MS (ESI positive mode) m/z 230 ($[M + H]^+$).

2-(2-Chloro-ethoxy)-3-methoxy-5-nitro-benzaldehyde (**9g**). The title compound was synthesized from 2-hydroxy-3-methoxy-5-nitro-benzaldehyde (**8e**) and 1,2-dichloroethane (yield, 64%). LC-MS (ESI positive mode) m/z 260 ($[M + H]^+$).

Following a procedure similar to that of **5e**, the following intermediates were synthesized:

(2-Methoxy-5-nitro-phenyl)-methanol (**10b**). The title compound was synthesized from 2-methoxy-3-nitrobenzaldehyde **8a** (yield, quantitative). LC-MS (ESI positive mode) m/z 184 ($[M + H]^+$).

(2-Morpholin-4-yl-5-nitro-phenyl)-methanol (**10c**). The title compound was synthesized from **9a** (yield, quantitative). LC-MS (ESI positive mode) m/z 239 ($[M + H]^+$).

4-(2-Hydroxymethyl-4-nitro-phenyl)-piperazine-1-carboxylic Acid tert-Butyl Ester (**10d**). The title compound was synthesized from **9b** (yield, quantitative). LC-MS (ESI positive mode) m/z 338 ($[M + H]^+$).

[2-(4-Methyl-piperazin-1-yl)-5-nitro-phenyl]-methanol (**10e**). The title compound was synthesized from **9c** (yield, quantitative). LC-MS (ESI positive mode) m/z 252 ($[M + H]^+$).

{2-[(2-Dimethylamino-ethyl)-methyl-amino]-5-nitro-phenyl}-methanol (**10f**). The title compound was synthesized from **9d** (yield, quantitative). LC-MS (ESI positive mode) m/z 254 ($[M + H]^+$).

[2-(2-Chloro ethoxy)-5-nitro-phenyl-methanol (**10g**). The title compound was synthesized from **9e** (yield, quantitative). LC-MS (ESI positive mode) m/z 232 ($[M + H]^+$); ^{1}H NMR (DMSO-d_6) δ 8.27−8.26 (m, 1H), 8.17 (dd, 1H), 7.19 (d, 1H), 4.60 (s, 2H), 4.44 (t, 2H), 4.00 (t, 2H); ^{13}C NMR (DMSO-d_6) δ 160.0, 141.4, 132.6, 124.4, 122.0, 111.8, 69.2, 57.5, 43.1.

[3-(2-Chloro-ethoxy)-5-nitro-phenyl]-methanol (**10h**). The title compound was synthesized from **9f** (yield, quantitative). LC-MS (ESI positive mode) m/z 232 ($[M + H]^+$);

[2-(2-Chloro-ethoxy)-3-methoxy-5-nitro-phenyl]-methanol (**10i**). The title compound was synthesized from **9g** (yield, quantitative). LC-MS (ESI positive mode) m/z 262 ($[M + H]^+$).

Following a procedure similar to that of **6a**, the following intermediates were synthesized:

1-Allyloxy-3-nitro-benzene (**11a**). The title compound was synthesized from **10a** and allyl bromide (yield, 62%). LC-MS (ESI positive mode) m/z 180 ($[M + H]^+$).

2-Allyloxymethyl-1-methoxy-4-nitro-benzene (**11b**). The title compound was synthesized from **10b** and allyl bromide (yield, 68%). LC-MS (ESI positive mode) m/z 224 ($[M + H]^+$).

4-(2-Allyloxymethyl-4-nitro-phenyl)-morpholine (**11c**). The title compound was synthesized from **10c** and allyl bromide (yield, 55%). LC-MS (ESI positive mode) m/z 279 ($[M + H]^+$).

4-(2-Allyloxymethyl-4-nitro-phenyl)-piperazine-1-carboxylic Acid tert-Butyl Ester (**11d**). The title compound was synthesized from **10d** and allyl bromide (yield, 60%). LC-MS (ESI positive mode) m/z 378 ($[M + H]^+$).

1-(2-Allyloxymethyl-4-nitro-phenyl)-4-methyl-piperazine (**11e**). The title compound was synthesized from **10e** and allyl bromide (yield, 48%). LC-MS (ESI positive mode) m/z 292 ($[M + H]^+$).

N-(2-Allyloxymethyl-4-nitro-phenyl)-N,N′,N′-trimethyl-ethane-1,2-diamine (**11f**). The title compound was synthesized from **10f** and allyl bromide (yield, 42%). LC-MS (ESI positive mode) m/z 294 ($[M + H]^+$); ^{1}H NMR ($CDCl_3$) δ 8.35 (d, 1H), 8.12 (dd, 1H), 7.09 (d, 1H), 6.01−5.94 (m, 1H), 5.37−5.24 (m, 2H), 4.53 (s, 2H), 4.13−4.11 (m, 2H), 3.63−3.59 (m, 2H), 2.90−2.84 (m, 2H), 2.88 (s, 3H), 2.60 (s, 6H).

*2-Allyloxymethyl-1-(2-chloro ethoxy)-4-nitro Benzene (**11g**).* The title compound was synthesized from **10g** and allyl bromide (yield, 63%). LC-MS (ESI positive mode) m/z 272 ($[M + H]^+$); ^{1}H NMR ($CDCl_3$) δ 8.37 (t, 1H), 8.17 (dd, 1H), 6.88 (dd, 1H), 6.04−5.91 (m, 1H), 5.43−5.21 (m, 2H), 4.35 (t, 2H), 4.15−4.13 (m, 2H), 3.87 (t, 2H); ^{13}C NMR ($CDCl_3$) δ 160.2, 142.0, 134.5, 129.1, 124.8, 124.2, 117.5, 110.7, 72.1, 68.9, 66.0, 41.7. Anal. Calcd. for $C_{12}H_{14}ClNO_4$: C, 53.05; H, 5.19; N, 5.16; Cl: 13.05. Found: C, 53.09; H, 5.30; N, 5.14; Cl, 13.37. IR (KBr pellet): 1593, 1519, 1341, 1270, 1077 cm^{-1}.

*1-Allyloxymethyl-3-(2-chloro-ethoxy)-5-nitro-benzene (**11h**).* The title compound was synthesized from **10h** and allyl bromide (yield, 59%). LC-MS (ESI positive mode) m/z 272 ($[M + H]^+$).

*1-Allyloxymethyl-2-(2-chloro-ethoxy)-3-methoxy-5-nitro-benzene (**11i**).* The title compound was synthesized from **10i** and allyl bromide (yield, 38%). LC-MS (ESI positive mode) m/z 302 ($[M + H]^+$).

*1-Allyloxymethyl-3,5-dinitro-benzene (**19**).* The title compound was synthesized from 3,5-dinitrobenzyl alcohol **18** and allyl bromide (yield, 41%). LC-MS (ESI positive mode) m/z 239 ($[M + H]^+$).

*1-[2-(2-Allyloxymethyl-4-nitro-phenoxy] Pyrrolidine (**11j**).* To a solution of **11g** (10 g, 36.8 mmol) in *N*,*N*-dimethylacetamide (DMA, 50 mL) was added pyrrolidine (20 mL, 2 vol), and the resulting mixture was stirred at 90 °C for 20 h. The reaction mixture was brought to rt and quenched with water (100 mL) and extracted in ethyl acetate (3 × 50 mL). The combined organic extracts were washed with water, brine, dried (Na_2SO_4), and concentrated under reduced pressure to afford the crude product **11m** (8.5 g; yield, 76%) as a pale yellow oil. LC-MS (ESI positive mode) m/z 307 ($[M + H]^+$); ^{1}H NMR ($CDCl_3$) δ 8.33 (d, 1H), 8.17 (dd, 1H), 6.91 (d, 1H), 6.03−5.93 (m, 1H), 5.37−5.23 (m, 2H), 4.56 (s, 2H), 4.26 (t, 2H), 4.12 (dt, 2H), 2.99 (t, 2H), 2.71−2.68 (m, 4H), 1.90−1.86 (m, 4H); ^{13}C NMR ($CDCl_3$) δ 161.0, 141.7, 134.6, 128.6, 125.0, 124.3, 117.6, 110.7, 72.2, 68.5, 66.3, 55.1, 54.7, 23.8.

*1-[2-(2-Allyloxymethyl-6-methoxy-4-nitro-phenoxy)-ethyl]-pyrrolidine (**11k**).* Following a similar procedure to that of **11i**, the title compound was synthesized from **11h** and pyrrolidine (yield, 66%). LC-MS (ESI positive mode) m/z 337 ($[M + H]^+$).

*1-But-3-enyloxy-3-nitro-benzene (**13**).* Following a similar procedure to that of **7**, the title compound was synthesized from **10a** and 4-bromo-but-1-ene (yield, 52%). LC-MS (ESI positive mode) m/z 194 ($[M + H]^+$).

*3-Allyloxy-phenylamine (**12a**).* Compound **11a** (1.0 g, 5.58 mmol) was taken in EtOH (10 mL, 10 vol), and fine Fe powder (0.93 g, 16.7 mmol) was added at 50−55 °C followed by NH_4Cl solution (1.76 g, 32 mmol in 2 mL water). The reaction mixture was refluxed for 4 h, and EtOH was removed from the reaction mixture under reduced pressure. The residue was basified with $NaHCO_3$ solution (pH 7−8) and extracted with CH_2Cl_2 (3 × 25 mL). The combined organic extracts were washed with brine, dried (Na_2SO_4), and concentrated under reduced pressure to furnish **12a** (0.75 g; yield, 90%) as a brown oil. This material was taken up for the next step without any purification. LC-MS (ESI positive mode) m/z 150 ($[M + H]^+$).

Following a procedure similar to that of **12a**, the following intermediates were synthesized:

*3-Allyloxymethyl-4-methoxy-phenylamine (**12b**).* The title compound was synthesized from **11b** (yield, 88%). LC-MS (ESI positive mode) m/z 194 ($[M + H]^+$).

*3-Allyloxymethyl-4-morpholin-4-yl-phenylamine (**12c**).* The title compound was synthesized from **11c** (yield, 83%). LC-MS (ESI positive mode) m/z 249 ($[M + H]^+$).

*4-(2-Allyloxymethyl-4-amino-phenyl)-piperazine-1-carboxylic Acid tert-Butyl Ester (**12d**).* The title compound was synthesized from **11d** (yield, 80%). LC-MS (ESI positive mode) m/z 348 ($[M + H]^+$). ^{1}H NMR ($CDCl_3$) δ 6.90 (d, 1H), 6.81 (d, 1H), 6.59 (dd, 1H), 6.00−5.93 (m, 1H), 5.34−5.29 (m, 2H), 4.55 (s, 2H), 4.07−4.05 (m, 2H), 3.55−3.50 (m, 4H), 2.78−2.72 (m, 4H), 1.48 (s, 9H).

*3-Allyloxymethyl-4-(4-methyl-piperazin-1-yl)-phenylamine (**12e**).* The title compound was synthesized from **11e** (yield, 76%). LC-MS (ESI positive mode) m/z 262 ($[M + H]^+$).

*2-Allyloxymethyl-N1-(2-dimethylamino-ethyl)-N1-methyl-benzene-1,4-diamine (**12f**).* The title compound was synthesized from **11f** (yield, 71%). LC-MS (ESI positive mode) m/z 264 ($[M + H]^+$); ^{1}H NMR ($CDCl_3$) δ 6.99 (d, 1H), 6.81 (d, 1H), 6.61 (dd, 1H), 6.00−5.93 (m, 1H), 5.34−5.19 (m, 2H), 4.51 (s, 2H), 4.07−4.05 (m, 2H), 3.58 (br, 2H), 3.28−3.24 (m, 2H), 2.81−2.60 (m, 2H), 2.60 (s, 3H), 2.51 (s, 6H).

*3-Allyloxymethyl-4-(2-chloro-ethoxy)-phenylamine (**12g**).* The title compound was synthesized from **11g** (yield, 86%). LC-MS (ESI positive mode) m/z 242 ($[M + H]^+$).

*3-Allyloxymethyl-5-(2-chloro-ethoxy)-phenylamine (**12h**).* The title compound was synthesized from **11h** (yield, 89%). LC-MS (ESI positive mode) m/z 242 ($[M + H]^+$).

*3-Allyloxymethyl-4-(2-pyrrolidin-1-yl-ethoxy)-phenylamine (**12j**).* The title compound was synthesized from **11j** (yield, 90%). LC-MS (ESI positive mode) m/z 277 ($[M + H]^+$); ^{1}H NMR (MeOD-d_4) δ 6.82−6.78 (m, 2H), 6.69 (dd, 1H), 5.93−5.83 (m, 1H), 5.26−5.11 (m, 2H), 4.45 (s, 2H), 4.20 (t, 2H), 3.97 (dt, 2H), 3.56 (t, 2H); ^{13}C NMR (MeOD-d_4) δ 149.4, 140.2, 134.7, 127.6, 118.2, 116.5, 116.2, 113.9, 70.8, 67.3, 64.6, 54.5, 54.1, 22.6. IR (KBr pellet): 1626, 1502, 1225, 1084, 798 cm^{-1}.

*3-Allyloxymethyl-5-methoxy-4-(2-pyrrolidin-1-yl-ethoxy)-phenylamine (**12k**).* The title compound was synthesized from **11k** (yield, 74%). LC-MS (ESI positive mode) m/z 307 ($[M + H]^+$).

*3-But-3-enyloxy-phenylamine (**14**).* The title compound was synthesized from **13** (yield, 89%). LC-MS (ESI positive mode) m/z 164 ($[M + H]^+$).

*5-Allyloxymethyl-benzene-1,3-diamine (**20**).* The title compound was synthesized from **19**, using twice the amount of Fe powder and NH_4Cl solution (yield, 73%). LC-MS (ESI positive mode) m/z 179 ($[M + H]^+$).

*(3-Allyloxymethyl-5-amino-phenyl)-carbamic acid 9H-fluoren-9-ylmethyl Ester (**12i**).* To a mixture of **20** (290 mg, 1.63 mmol) and Fmoc-Cl (350 mg, 1.35 mmol) in 1,2-dioxane was added di-isopropylethylamine (0.5 mL), and the resulting mixture was stirred at rt for 2 h. The reaction mixture was concentrated under reduced pressure to furnish an oil, which was purified by column (40% EtOAc/*n*-hexane) to obtain 370 mg of **12k** (yield, 95%). LC-MS (ESI positive mode) m/z 401 ($[M + H]^+$).

*(3-But-3-enyloxy-phenyl)-[4-(3-but-3-enyloxy-phenyl)-pyrimidin-2-yl]-amine (**15a**).* To a mixture of **7** (100 mg, 0.38 mmol) and **14** (75 mg, 0.46 mmol) in *n*-butanol (2 mL) at ambient temperature was added 4 M HCl (0.5 mL), and the resulting mixture was stirred at 80 °C for 4 h. The reaction mixture was cooled to 0 °C and quenched with water. The product was extracted with CH_2Cl_2 thrice, and the combined organic extracts were washed with saturated $NaHCO_3$ followed by brine, dried over Na_2SO_4, and concentrated under reduced pressure to furnish an oil, which was purified by column (EtOAc/*n*-hexane) to obtain 71 mg of **15a** (yield, 48%). LC-MS (ESI positive mode) m/z 388 ($[M + H]^+$).

Following a procedure similar to that of **15a**, the following intermediates were synthesized:

*(3-Allyloxy-phenyl)-[4-(3-but-3-enyloxy-phenyl)-pyrimidin-2-yl]-amine (**15b**).* The title compound was synthesized from **7** and **12a** (yield, 21%). LC-MS (ESI positive mode) m/z 374 ($[M + H]^+$).

*(3-Allyloxymethyl-4-methoxy-phenyl)-[4-(3-but-3-enyloxy-phenyl)-pyrimidin-2-yl]-amine (**15c**).* The title compound was synthesized from **7** and **12b** (yield, 26%). LC-MS (ESI positive mode) m/z 418 ($[M + H]^+$).

*(3-Allyloxymethyl-4-methoxy-phenyl)-[4-(3-allyloxy-phenyl)-pyrimidin-2-yl]-amine (**15d**).* The title compound was synthesized from **6a** and **12b** (yield, 51%). LC-MS (ESI positive mode) m/z 404 ($[M + H]^+$).

*(3-Allyloxymethyl-4-methoxy-phenyl)-[4-(3-allyloxymethyl-phenyl)-pyrimidin-2-yl]-amine (**15e**).* The title compound was synthesized from **6b** and **12b** (yield, 56%). LC-MS (ESI positive mode) m/z 418 ($[M + H]^+$).

*(3-Allyloxymethyl-4-morpholin-4-yl-phenyl)-[4-(3-allyloxymethyl-phenyl)-pyrimidin-2-yl]-amine (**15f**).* The title compound was synthesized from **6b** and **12c** (yield, 78%). LC-MS (ESI positive mode) *m/z* 473 ($[M + H]^+$).

*4-{2-Allyloxymethyl-4-[4-(3-allyloxymethyl-phenyl)-pyrimidin-2-ylamino]-phenyl}-piperazine-1-carboxylic Acid tert-Butyl Ester (**15g**).* The title compound was synthesized from **6b** and **12d** (yield, 86%). LC-MS (ESI positive mode) *m/z* 572 ($[M + H]^+$).

*[3-Allyloxymethyl-4-(4-methyl-piperazin-1-yl)-phenyl]-[4-(3-allyloxymethyl-phenyl)-pyrimidin-2-yl]-amine (**15h**).* The title compound was synthesized from **6b** and **12e** (yield, 88%). LC-MS (ESI positive mode) *m/z* 486 ($[M + H]^+$).

*2-Allyloxymethyl-N4-[4-(3-allyloxymethyl-phenyl)-pyrimidin-2-yl]-N1-(2-dimethylamino-ethyl)-N1-methyl-benzene-1,4-diamine (**15i**).* The title compound was synthesized from **6b** and **12f** (yield, 71%). LC-MS (ESI positive mode) *m/z* 488 ($[M + H]^+$).

*[3-Allyloxymethyl-4-(2-chloro-ethoxy)-phenyl]-[4-(3-allyloxymethyl-phenyl)-pyrimidin-2-yl]-amine (**15j**).* The title compound was synthesized from **6b** and **12g** (yield, 92%). LC-MS (ESI positive mode) *m/z* 466 ($[M + H]^+$).

*[3-Allyloxymethyl-5-(2-chloro-ethoxy)-phenyl]-[4-(3-allyloxymethyl-phenyl)-pyrimidin-2-yl]-amine (**15k**).* The title compound was synthesized from **6b** and **12h** (yield, 82%). LC-MS (ESI positive mode) *m/z* 466 ($[M + H]^+$).

*{3-Allyloxymethyl-5-[4-(3-allyloxymethyl-phenyl)-pyrimidin-2-ylamino]-phenyl}-carbamic Acid 9H-Fluoren-9-yl-methyl Ester (**15l**).* The title compound was synthesized from **6b** and **12i** (yield, 90%). LC-MS (ESI positive mode) *m/z* 625 ($[M + H]^+$).

*[3-Allyloxymethyl-5-methoxy-4-(2-pyrrolidin-1-yl-ethoxy)-phenyl]-[4-(3-allyloxymethyl-phenyl)-pyrimidin-2-yl]-amine (**15m**).* The title compound was synthesized from **6b** and **12k** (yield, 21%) LC-MS (ESI positive mode) *m/z* 531 ($[M + H]^+$).

*[4-(3-Allyloxymethyl-phenyl)-5-methyl-pyrimidin-2-yl]-[3-allyloxymethyl-4-(2-pyrrolidin-1-yl-ethoxy)-phenyl]-amine (**15n**).* The title compound was synthesized from **6g** and **12j** (yield, 65%). LC-MS (ESI positive mode) *m/z* 515 ($[M + H]^+$).

*[4-(3-Allyloxymethyl-phenyl)-5-fluoro-pyrimidin-2-yl]-[3-allyloxymethyl-4-(2-pyrrolidin-1-yl-ethoxy)-phenyl]-amine (**15o**).* The title compound was synthesized from **6h** and **12j** (yield, 65%). LC-MS (ESI positive mode) *m/z* 519 ($[M + H]^+$).

*[4-(5-Allyloxymethyl-2-methoxy-phenyl)-pyrimidin-2-yl]-[3-allyloxymethyl-4-(2-pyrrolidin-1-yl-ethoxy)-phenyl]-amine (**15p**).* The title compound was synthesized from **6f** and **12j** (yield, 91%). LC-MS (ESI positive mode) *m/z* 531 ($[M + H]^+$).

*[4-(3-Allyloxymethyl-5-fluoro-phenyl)-pyrimidin-2-yl]-[3-allyloxymethyl-4-(2-pyrrolidin-1-yl-ethoxy)-phenyl]-amine (**15q**).* The title compound was synthesized from **6e** and **12j** (yield, 47%). LC-MS (ESI positive mode) *m/z* 519 ($[M + H]^+$).

*[4-(3-Allyloxymethyl-4-methoxy-phenyl)-pyrimidin-2-yl]-[3-allyloxymethyl-4-(2-pyrrolidin-1-yl-ethoxy)-phenyl]-amine (**15r**).* The title compound was synthesized from **6d** and **12j** (yield, 81%). LC-MS (ESI positive mode) *m/z* 531 ($[M + H]^+$).

*[4-(3-Allyloxymethyl-4-fluoro-phenyl)-pyrimidin-2-yl]-[3-allyloxymethyl-4-(2-pyrrolidin-1-yl-ethoxy)-phenyl]-amine (**15s**).* The title compound was synthesized from **6c** and **12j** (yield, 39%). LC-MS (ESI positive mode) *m/z* 519 ($[M + H]^+$).

*(**16a**).* To **15a** (20 mg, 0.052 mmol) in CH_2Cl_2 (50 mL) at ambient temperature was added 4 M HCl until the pH reached 2.0−2.2. The solution was degassed (N_2), and Grubbs second generation catalyst (7 mg, 0.005 mmol) was added in two portions at 1 h intervals. The resulting mixture was stirred at 40−45 °C for 4 h. The reaction mixture was cooled and concentrated under reduced pressure to furnish an oil, which was purified by preparative HPLC to obtain 9 mg of **16a** (yield, 48%, >95% trans by NMR). LC-MS (ESI positive mode) *m/z* 360 ($[M + H]^+$); ^{1}H NMR (DMSO-d_6) δ 9.77 (s, 1H), 8.57 (d, 1H), 8.48 (t, 1H), 8.09 (t, 1H), 7.65 (d, 1H), 7.46 (d, 1H), 7.44 (t, 1H), 7.17 (t, 1H), 7.10 (dd, 1H), 6.84 (dd, 1H), 6.54 (dd, 1H), 5.60−5.68 (m, 2H), 4.12 (t, 2H), 4.06 (t, 2H), 2.56−2.61 (m, 4H).

Following a procedure similar to that of **16a**, the following compounds were synthesized:

*(**16b**).* The title compound was synthesized from **15b** (yield, 51%; >95% *trans* by NMR). LC-MS (ESI positive mode) *m/z* 346 ($[M + H]^+$). ^{1}H NMR ($CDCl_3$): δ 11.30 (s, 1H), 8.29 (d, 1H), 8.21 (t, 1H), 8.11 (t, 1H), 7.57 (d, 1H), 7.48 (t, 1H), 7.32−7.35 (m, 2H), 7.22−7.25 (m, 1H), 6.95 (dd, 1H), 6.82 (dd, 1H), 6.02−6.08 (m, 1H), 5.87−5.93 (m, 1H), 4.78 (d, 2H), 4.29 (t, 2H), 2.63−2.68 (m, 2H).

*(**16c**).* The title compound was synthesized from **15c** (yield, 45%; >95% *trans* by NMR). LC-MS (ESI positive mode) *m/z* 390 ($[M + H]^+$); ^{1}H NMR.

*(**16d**).* The title compound was synthesized from **15d** (yield, 45%; >95% *trans* by NMR). LC-MS (ESI positive mode) *m/z* 502 ($[M + H]^+$). ^{1}H NMR ($CDCl_3$): δ 11.76 (s, 1H), 8.16 (d, 1H), 8.14 (d, 1H), 7.66 (s, 1H), 7.40−7.42 (m, 2H), 7.28 (dd, 1H), 7.19−7.21 (m, 1H), 7.17 (d, 1H), 6.90 (d, 1H), 6.07−6.14 (m, 1H), 5.82−5.88(m, 1H), 5.67 (d, 2H), 4.60 (s, 2H), 4.14 (dd, 2H), 3.86 (s, 3H).

*(**16e**).* The title compound was synthesized from **15e** (yield, 48%; mixture of *trans/cis* 80:20 by NMR). LC-MS (ESI positive mode) *m/z* 390 ($[M + H]^+$). ^{1}H NMR (DMSO-d_6): δ 9.55 (s, 1H), 8.54−8.52 (m, 2H), 8.19 (s, 1H), 8.02 (d, 1H), 7.56 (dd, 1H), 7.40 (d, 1H), 7.15 (d, 1H), 6.98 (d, 1H), 5.84−5.72 (m, 2H), 4.57 (s, 2H), 4.49 (s, 2H), 4.06 (d, 2H), 4.01 (d, 2H), 3.78 (s, 3H). ^{13}C NMR (DMSO-d_6): δ 63.4, 160.7, 159.8, 152.5, 139.1, 137.3, 134.2, 131.5, 131.2, 130.3, 129.6, 127.0, 126.9, 126.2, 121.2, 120.1, 111.9, 107.8, 69.6, 69.3, 67.5, 65.7, 56.1.

*(**17a**).* The title compound was synthesized from **15f** (yield, 43%; mixture of *trans/cis* 85:15 by NMR). LC-MS (ESI positive mode) *m/z* 502 ($[M + H]^+$). ^{1}H NMR ($CDCl_3$): δ 11.56 (s, 1H), 8.45 (d, 1H), 8.29−8.27 (m, 1H), 8.22 (d, 1H), 7.90 (d, 1H), 7.76 (d, 1H), 7.59 (t, 1H), 7.31 (d, 1H), 7.26−7.21 (m, 1H), 7.10 (d, 1H), 5.91−5.69 (m, 2H), 4.66 (s, 2H), 4.64 (s, 2H), 4.17−4.15 (m, 2H), 4.06−4.04 (m, 2H), 3.89−3.82 (m, 4H), 2.30−2.96 (m, 4H).

*(**17b**).* The title compound was synthesized from **15g** using 10 mol % Zhan catalyst-1B instead of the Grubbs second generation catalyst (yield, 96%, isomers ration not determined). LC-MS (ESI positive mode) *m/z* 502 ($[M + H]^+$).

*(**17d**).* The title compound was synthesized from **15h** (yield, 52%; mixture of *trans/cis* 80:20 by NMR). LC-MS (ESI positive mode) *m/z* 502 ($[M + H]^+$). ^{1}H NMR ($CDCl_3$): δ 10.62 (s, 1H), 8.59 (d, 1H), 8.29−8.24 (m, 2H), 7.88 (d, 1H), 7.72 (d, 1H), 7.59−7.56 (m, 1H), 7.30 (d, 1H), 7.18−7.10 (m, 2H), 5.90−5.69 (m, 2H), 4.65 (s, 2H), 4.61 (s, 2H), 4.17−4.15 (m, 2H), 4.08−4.06 (m, 2H), 3.68−3.66 (m, 2H), 3.37−3.25 (m, 4H), 2.93−2.91 (m, 2H), 2.90 (s, 3H).

*(**17h**).* The title compound was synthesized from **15i** (yield, 56%; mixture of *trans/cis* 85:15 by NMR). LC-MS (ESI positive mode) *m/z* 502 ($[M + H]^+$). ^{1}H NMR (MeOD-d_4): δ 8.87 (s, 1H), 8.48 (s, 1H), 8.29 (s, 1H), 7.98 (d, 1H), 7.64 (d, 1H), 7.54 (d, 1H), 7.40 (d, 1H), 7.37 (d, 1H), 7.20 (dd, 1H), 6.00−5.78 (m, 2H), 4.67 (s, 2H), 4.27 (d, 2H), 4.06 (d, 2H), 3.40 (t, 2H), 3.15 (t, 2H), 2.89 (s, 6H), 2.76 (s, 3H).

*(**21a**).* The title compound was synthesized from **15j** (yield, 74%; mixture of *trans/cis* 85:15 by NMR). LC-MS (ESI positive mode) *m/z* 438 ($[M + H]^+$). ^{1}H NMR ($CDCl_3$): δ 8.70 (d, 1H), 8.43 (d, 1H), 8.30 (s, 1H), 7.81 (d, 1H), 7.61−7.59 (m, 1H), 7.50 (t, 1H), 7.17−7.15 (m, 2H), 6.85−6.82 (m, 2H), 5.91−5.79 (m, 2H), 4.66 (s, 2H), 4.65 (s, 2H), 4.27 (t, 2H), 4.17 (d, 2H), 4.07 (d, 2H), 3.83 (t, 2H). ^{13}C NMR (DMSO-d_6): δ 163.4, 160.7, 159.9, 151.1, 139.1, 137.2, 134.9, 131.5, 131.3, 130.4, 129.6, 127.4, 127.0 (duplicate), 121.0, 120.1, 114.4, 107.9, 69.8, 69.7, 69.4, 67.5, 65.5, 43.8.

*(**21g**).* The title compound was synthesized from **15k** (yield, 56%; mixture of *trans/cis* 80:20 by NMR). LC-MS (ESI positive mode) *m/z*

438 ([M + H]$^+$). ^{1}H NMR ($CDCl_3$): δ 8.46 (d, 1H), 8.43 (s, 1H), 8.39 (s, 1H), 7.83 (d, 1H), 7.58−7.54 (m, 2H), 7.51−7.49 (m, 1H), 7.21 (d, 1H), 6.70 (s, 1H), 6.49 (t, 1H), 5.92−5.81 (m 2H), 4.63 (s, 2H), 4.56 (s, 2H), 4.27 (t, 2H), 4.15 (d, 2H), 4.09 (d, 2H), 3.83 (t, 2H).

(***21j***). The title compound was synthesized from **15l** using 10 mol % Zhan catalyst-1B instead of the Grubbs second generation catalyst (yield, 73%; mixture of *trans*/*cis* 85:15 by NMR). LC-MS (ESI positive mode) *m*/*z* 597 ([M + H]$^+$).

(***22a***). The title compound was synthesized from **15m** (yield, 43%; mixture of *trans*/*cis* 80:20 by NMR). LC-MS (ESI positive mode) *m*/*z* 503 ([M + H]$^+$). ^{1}H NMR ($CDCl_3$): δ 8.33−8.28 (m, 2H), 8.10 (d, 1H), 7.93 (d, 1H), 7.79 (d, 1H), 7.63 (t, 1H), 7.40 (d, 1H), 6.93 (d, 1H), 5.94−5.82 (m, 2H), 4.68 (s, 1H), 4.60 (s, 2H), 4.36 (m, 2H), 4.18 (d, 2H), 4.11 (d, 2H), 4.12−4.03 (m, 2H), 3.94 (s, 3H), 3.63(m, 2H), 3.19 (m, 2H), 2.34−2.22 (m, 4H).

(***22b***). The title compound was synthesized from **15n** (yield, 79%; mixture of *trans*/*cis* 88:12 by NMR). LC-MS (ESI positive mode) *m*/*z* 487 ([M + H]$^+$). ^{1}H NMR ($CDCl_3$): δ 10.4 (s, 1H), 8.40 (s, 1H), 8.12 (s, 1H), 7.78 (s, 1H), 7.65−7.36 (m, 3H), 7.07 (d, 1H), 6.78 (d, 1H), 5.84−5.64 (m, 2H), 4.56 (s, 2H), 4.42 (s, 2H), 4.31 (br s, 2H), 4.10 (d, 2H), 3.99 (d, 2H), 3.85 (m, 2H), 3.50 (m, 2H), 2.97 (m, 2H), 2.26 (s, 3H), 2.05 (m, 4H).

(***22c***). The title compound was synthesized from **15o** (yield, 56%; mixture of *trans*/*cis* 80:20 by NMR). LC-MS (ESI positive mode) *m*/*z* 491 ([M + H]$^+$). ^{1}H NMR ($CDCl_3$): δ 8.23 (m, 1H), 8.12 (s, 1H), 7.95 (d, 1H), 7.52 (d, 1H), 7.42 (m, 1H), 7.12 (s, 1H), 6.76 (d, 2H), 5.75 (m, 2H), 4.59 (s, 2H), 4.47 (m, 2H), 4.14 (m, 2H), 4.05 (m, 2H), 4.01 (m, 2H), 2.96 (m, 2H), 2.71 (m, 4H), 1.79 (m, 4H).

(***22d***). The title compound was synthesized from **15p** (yield, 32%; mixture of *trans*/*cis* 85:15 by NMR). LC-MS (ESI positive mode) *m*/*z* 503 ([M + H]$^+$). ^{1}H NMR (MeOD-d_4): δ 8.61 (d, 1H), 8.36 (d, 1H), 8.07 (s, 1H), 7.59 (d, 1H), 7.53 (dd, 1H), 7.19 (d, 1 H), 7.13 (dd, 1H), 7.04 (d, 1H), 5.90 (dt, 1H), 5.79 (dt, 1H), 4.61 (s, 2H), 4.59 (s, 2H), 4.37 (t, 2H), 4.11 (d, 2H), 4.08 (d, 2H), 3.95 (s, 3H), 3.80 (m, 2H); 3.68 (t, 2H), 2.17 (m, 2H), 2.08 (m, 2H), 1.30 (m, 2H).

(***22e***). The title compound was synthesized from **15q** (yield, 42%; mixture of *trans*/*cis* 80:20 by NMR). LC-MS (ESI positive mode) *m*/*z* 491 ([M + H]$^+$). ^{1}H NMR (MeOD-d_4): δ 8.72 (d, 1H), 8.48 (m, 1H), 8.11 (s, 1H), 7.72 (m, 1H), 7.34 (m, 2H), 7.05−7.15 (m, 2H), 5.82−5.90 (m, 2H), 4.65 (m, 2H), 4.39 (m, 2H), 4.16 (m, 2H), 4.09 (m, 2H), 3.80 (m, 2H), 3.71 (m, 2H), 3.27 (m, 4H), 2.08−2.24 (m, 4H).

(***22f***). The title compound was synthesized from **15r** (yield, 48%; mixture of *trans*/*cis* 80:20 by NMR). LC-MS (ESI positive mode) *m*/*z* 503 ([M + H]$^+$). ^{1}H NMR (MeOD-d_4): δ 8.50−8.48 (m, 1H), 8.37 (d, 1H), 8.27 (d, 1H), 8.07 (dd, 1H), 7.38 (d, 1H), 7.17−7.15 (m, 2H), 7.08−7.06 (m, 1H), 5.98−5.86 (m, 2H), 4.69 (s, 2H), 4.64 (s, 2H), 4.39 (t, 2H), 4.17 (d, 2H), 4.08 (d, 2H), 3.88−3.82 (m, 2H), 3.70 (t, 2H), 2.23−2.21 (m, 2H), 2.10−2.07 (m, 2H).

(***22g***). The title compound was synthesized from **15s** (yield, 49%; mixture of *trans*/*cis* 80:20 by NMR). LC-MS (ESI positive mode) *m*/*z* 491 ([M + H]$^+$). ^{1}H NMR (MeOD-d_4): δ 8.45 (m, 2H), 8.30 (m, 1H), 8.05 (m, 1H), 7.38 (m, 1H), 7.26 (m, 1H), 7.16 (m, 1H), 7.08 (m, 1H), 5.90−5.92 (m, 2H), 4.65 (m, 4H), 4.39 (m, 2H), 4.16 (m, 2H), 4.09 (m, 2H), 3.85 (m, 2H), 3.71 (m, 2H), 3.32 (m, 2H), 2.08−2.25 (m, 4H).

(***16f***). To a mixture of **16e** (20 mg, 0.051 mmol) in DMF (2 mL) was added sodium ethanethiolate (5 mg, 0.061 mmol), and the resulting mixture was stirred at 120 °C for 20 h. It was cooled, and saturated NH_4Cl was added. The product was extracted with CH_2Cl_2 thrice, and the combined organic extracts were dried over Na_2SO_4 and concentrated under reduced pressure to furnish an oil which was further purified by preparative HPLC to furnish **16f** (6 mg; yield, 30%; mixture of *trans*/*cis* 80:20 by NMR). LC-MS (ESI positive mode) *m*/*z* 376 ([M + H]$^+$). ^{1}H NMR (DMSO-d_6): δ 9.43 (s, 1H), 9.11 (br, 1H), 8.50 (d, 1H), 8.44 (d, 1H), 8.20 (s, 1H), 8.01 (dd, 1H), 7.56−7.54 (m, 2H), 7.37 (d, 1H), 6.99 (dd, 1H), 6.76 (d, 1H), 5.85−5.73 (m, 2H), 4.56 (s, 2H), 4.47 (s, 2H), 4.06 (s, 2H), 4.01 (d, 2H). ^{13}C NMR (DMSO-d_6): δ 163.3, 160.7, 159.8, 150.6, 139.1, 137.3, 132.8, 131.6, 131.2, 130.3, 129.6, 127.1, 126.9, 124.3, 121.3, 120.3, 115.8, 107.5, 169.5, 69.4, 67.6, 66.0.

(***17c***). To a mixture of **17b** (131 mg, 0.241 mmol) in CH_2Cl_2 (5 mL) was added TFA (0.5 mL), and the resulting mixture was stirred at 40 °C for 2 h. It was cooled and concentrated under reduced pressure. The crude product was further purified by preparative HPLC to furnish **17c** (70 mg; yield, 73%; mixture of *trans*/*cis* 80:20 by NMR) as a pale yellow solid. LC-MS (ESI positive mode) *m*/*z* 444 ([M + H]$^+$). ^{1}H NMR (MeOD-d_4): δ 8.77 (d, 1H), 8.46 (d, 1H), 8.31 (s, 1H), 8.00 (d, 1H), 7.65−7.63 (m, 1H), 7.56 (t, 1H), 7.41 (d, 1H), 7.19 (d, 1H), 7.11 (dd, 1H), 5.95−5.76 (m, 2H), 4.68 (s, 2H), 4.67 (s, 2H), 4.17 (d, 2H), 4.07 (d, 2H), 3.42−3.38 (m, 4H), 3.25−3.21 (m, 4H).

(***17e***). To a mixture of **17c** (16 mg, 0.036 mmol) and 2-bromoethanol (5 μL, 0.072 mmol) in CH_2Cl_2 (1 mL) was added Et_3N (14 μL, 0.10 mmol), and the resulting mixture was stirred at rt for 2 h. It was concentrated under reduced pressure and further purified by preparative HPLC to furnish **17e** (6 mg; yield, 34%; mixture of *trans*/*cis* 80:20 by NMR) as a pale yellow solid. LC-MS (ESI positive mode) *m*/*z* 488 ([M + H]$^+$). ^{1}H NMR ($CDCl_3$): δ 11.76 (s, 1H), 8.51 (d, 1H), 8.26 (s, 1H), 8.23 (d, 1H), 7.90 (d, 1H), 7.76 (d, 1H), 7.62 (t, 1H), 7.34 (d, 1H), 7.30−7.27 (m, 1H), 7.15 (d, 1H), 5.90−5.73 (m, 2H), 4.65 (s, 2H), 4.60 (s, 2H), 4.14 (d, 2H), 4.07 (d, 4H), 3.83−3.80 (m, 2H), 3.40−3.38 (m, 2H), 3.30−3.27 (m, 4H), 3.17−3.13 (m, 2H).

(***17f***). To a mixture of **17c** (9 mg, 0.020 mmol) and acetyl chloride (3 μL, 0.041 mmol) in CH_2Cl_2 (1 mL) was added Et_3N (9 μL, 0.060 mmol), and the resulting mixture was stirred at rt for 2 h. It was concentrated under reduced pressure and further purified by preparative HPLC to furnish **17f** (6 mg; yield, 63%; mixture of *trans*/*cis* 80:20 by NMR). LC-MS (ESI positive mode) *m*/*z* 486 ([M + H]$^+$). ^{1}H NMR ($CDCl_3$): δ 12.00 (s, 1H), 8.46 (d, 1H), 8.28 (s, 1H), 8.25 (d, 1H), 7.92 (d, 1H), 7.78 (d, 1H), 7.59 (t, 1H), 7.36 (d, 1H), 7.31−7.28 (m, 1H), 7.09 (d, 1H), 5.91−5.75 (m, 2H), 4.67 (s, 2H), 4.65 (s, 2H), 4.17 (d, 2H), 4.07 (d, 2H), 3.83−3.67 (m, 4H), 3.06−2.93 (m, 4H), 2.22 (s, 3H).

(***17g***). To a mixture of **17c** (14 mg, 0.032 mmol) and ethanesulfonyl chloride (6 μL, 0.063 mmol) in THF (1 mL) was added K_2CO_3 (10 mg, 0.072 mmol), and the resulting mixture was stirred at 70 °C for 4 h. It was cooled and concentrated under reduced pressure. The crude product was further purified by preparative HPLC to furnish **17g** (7 mg; yield, 41%; mixture of *trans*/*cis* 80:20 by NMR) as a pale yellow solid. LC-MS (ESI positive mode) *m*/*z* 536 ([M + H]$^+$). ^{1}H NMR ($CDCl_3$): δ 8.50 (d, 1H), 8.29 (s, 1H), 8.22 (d, 1H), 7.90 (d, 1H), 7.75 (d, 1H), 7.57 (t, 1H), 7.32 (d, 1H), 7.25−7.21 (m, 1H), 7.10 (d, 1H), 5.90−5.73 (m, 2H), 4.65 (s, 2H), 4.64 (s, 2H), 4.15 (d, 2H), 4.06 (d, 2H), 3.07−2.99 (m, 4H), 3.02 (d, 2H), 3.25−3.21 (m, 4H), 1.45 (t, 3H).

(***21b***). To a microwave glass vial was added **21a** (20 mg, 0.046 mmol), diethylamine (10 μL, 0.11 mmol), and DMA (1 mL), and the resulting mixture was stirred under microwave conditions at 80 °C for 30 min. The mixture was diluted with MeOH and purified directly by preparative HPLC to furnish **21b** (18 mg; yield, 82%; mixture of *trans*/*cis* 85:15 by NMR) as a pale yellow solid. LC-MS (ESI positive mode) *m*/*z* 475 ([M + H]$^+$). ^{1}H NMR (MeOD-d_4): δ 8.49 (s, 1H), 7.98−7.97 (m, 1H), 7.77 (s, 1H), 7.63−7.61 (m, 1H), 7.57−7.55 (m, 1H), 7.42−7.38 (m, 4H), 7.14−7.11 (m, 1H), 5.83−5.76 (m, 1H), 5.42−5.34 (m, 1H), 4.29−4.27 (m, 1H), 4.13−4.10 (m, 2H), 3.83−3.72 (m, 2H), 3.24 (s, 2H), 3.25−2.97 (m, 4H), 2.29−2.24 (m, 2H), 2.11−1.92 (m, 4H).

Following a procedure similar to that of **21b**, the following compounds were synthesized:

(***21c***). The title compound was synthesized from **21a** and pyrrolidine (yield, 83%; mixture of *trans*/*cis* 85:15 by NMR). LC-MS (ESI positive mode) *m*/*z* 473 ([M + H]$^+$). HRMS: theoretical $C_{28}H_{32}N_4O_3$ MW, 472.2474; found, 473.2547. ^{1}H NMR (MeOD-d_4): δ 8.79 (d, 1H), 8.46 (d, 1H), 8.34−8.31 (m, 1H, CH), 7.98−7.96 (m, 1H), 7.62−7.49 (m, 2H),

7.35 (d, 1H), 7.15−7.10 (m, 1H), 7.07−7.02 (m, 1H), 5.98−5.75 (m, 2H), 4.67 (s, 2H), 4.67 (s, 2H), 4.39−4.36 (m, 2H), 4.17 (d, 2H), 4.08 (d, 2H), 3.88−3.82 (m, 2H), 3.70 (t, 2H), 2.23−2.21 (m, 2H), 2.10−2.07 (m, 2H); chloride content (titration) 7.7% (1.18 equivs); water content (Karl Fischer) 6.1% (1.85 equivs); Anal. Calcd. for $C_{28}H_{32}N_4O_3 \cdot 1.18\,HCl \cdot 1.85H_2O$: C, 61.46; H, 6.46; N, 10.24; Cl, 7.65. Found: C, 61.99; H, 6.91; N, 10.25; Cl, 7.45.

(***21d***). The title compound was synthesized from **21a** and piperidine (yield, 84%; mixture of *trans*/*cis* 85:15 by NMR). LC-MS (ESI positive mode) *m*/*z* 487 ($[M + H]^+$). ^{1}H NMR (MeOD-d_4): δ 8.65 (d, 1H), 8.33 (d, 1H), 8.15 (s, 1H), 7.84 (d, 1H), 7.44 (m, 2H), 7.22 (d, 1H), 7.00 (m, 1H), 6.93 (d, 1H), 5.82−5.66 (m, 2H), 4.52 (s, 2H), 4.50 (s, 2H), 4.30 (t, 2H), 4.02 (d, 2H), 3.95 (d, 2H), 3.61 (br, 2H), 3.49 (t, 2H), 3.03 (m, 2H), 1.98 (m, 2H), 1.77 (m, 4H). ^{13}C NMR (MeOD-d_4): δ 159.6, 152.8, 140.2, 138.6, 132.5, 132.4, 132.1, 130.4, 128.7, 128.0, 127.7, 123.0, 121.2, 114.6, 109.0, 70.8, 70.6, 68.9, 67.7, 64.7, 57.6, 55.3, 24.4, 22.7.

(***21e***). The title compound was synthesized from **21a** and 2-pyrrolidinone (yield, 72%; mixture of *trans*/*cis* 85:15 by NMR). LC-MS (ESI positive mode) *m*/*z* 487 ($[M + H]^+$). ^{1}H NMR (DMSO-d_6): δ 9.55 (s, 1H), 8.57 (s, 1H), 8.52 (d, 1H), 8.19 (s, 1H), 8.01 (d, 1H), 7.56 (m, 2H), 7.39 (d, 1H), 7.13 (dd, 1H), 6.96 (d, 1H), 5.88−5.69 (m, 2H), 4.57 (s, 2H), 4.47 (s, 2H), 4.09 (m, 6H), 3.58 (t, 2H), 3.51 (t, 2H), 2.24 (t, 2H), 1.95 (t, 2H).

(***21f***). The title compound was synthesized from **21a** and 3-pyrrolidinone (yield, 75%; mixture of *trans*/*cis* 85:15 by NMR). LC-MS (ESI positive mode) *m*/*z* 487 ($[M + H]^+$). ^{1}H NMR (DMSO-d_6): δ 9.55 (s, 1H), 8.57 (s, 1H), 8.52 (d, 1H), 8.19 (s, 1H), 8.01 (d, 1H), 7.56 (m, 2H), 7.39 (d, 1H), 7.13 (dd, 1H), 6.97 (d, 1H), 5.87−5.69 (m, 2H), 4.56 (s, 2H), 4.48 (s, 2H), 4.11 (t, 2H), 4.03 (m, 4H), 3.08 (s, 2H), 2.99 (t, 2H), 2.92 (t, 2H), 2.34 (t, 2H).

(***21h***). The title compound was synthesized from **21g** and pyrrolidine (yield, 90%; mixture of *trans*/*cis* 80:20 by NMR). LC-MS (ESI positive mode) *m*/*z* 473 ($[M + H]^+$). ^{1}H NMR (MeOD-d_4): δ 8.47 (d, 1H), 8.35 (d, 2H), 8.00 (d, 1H), 7.62−7.59 (m, 1H), 7.56−7.52 (m, 1H), 7.43 (d, 1H), 6.80−6.79 (m, 1H), 6.75−6.74 (m, 1H), 5.92−5.79 (m, 2H), 4.61 (s, 2H), 4.57 (s, 2H), 4.37 (t, 2H), 4.15 (d, 2H), 4.08 (d, 2H), 3.77−3.72 (m, 2H), 3.68 (t, 2H), 3.26−3.21 (m, 2H), 2.23−2.16 (m, 2H), 2.11−2.03 (m, 2H).

(***21i***). The title compound was synthesized from **21g** and morpholine (yield, 79%; mixture of *trans*/*cis* 80:20 by NMR). LC-MS (ESI positive mode) *m*/*z* 489 ($[M + H]^+$). ^{1}H NMR (MeOD-d_4): δ 8.47 (d, 1H), 8.36 (d, 2H), 8.00 (d, 1H), 7.62−7.60 (m, 1H), 7.55−7.51 (m, 1H), 7.42 (d, 1H), 6.80−6.79 (m, 1H), 6.75−6.73 (m, 1H), 5.92−5.79 (m, 2H), 4.61 (s, 2H), 4.56 (s, 2H), 4.43 (t, 2H), 4.15 (d, 2H), 4.08 (d, 2H), 4.08−4.04 (m, 2H), 3.90−3.79 (m, 2H), 3.66 (t, 2H), 3.65−3.58 (m, 2H).

(***21k***). To a mixture of **21j** (156 mg, 0.261 mmol) in CH_2Cl_2 (5 mL) was added piperidine (1 mL, 20% v/v), and the resulting mixture was stirred at rt for 30 min. It was concentrated under reduced pressure and purified by preparative HPLC to furnish **21k** (80 mg; yield, 82%; mixture of *trans*/*cis* 85:15 by NMR) as a pale yellow solid. LC-MS (ESI positive mode) *m*/*z* 375 ($[M + H]^+$). ^{1}H NMR (MeOD-d_4): δ 8.83 (s, 1H), 8.53 (d, 1H), 8.34 (s, 1H), 7.99 (dd, 1H), 7.61−7.56 (m, 1H), 7.54−7.51 (m, 1H), 7.45 (d, 1H), 7.08−7.06 (m, 2H), 5.94−5.81 (m, 2H), 4.63 (s, 4H), 4.18 (d, 2H), 4.10 (d, 2H).

(***21l***). To a mixture of **21k** (20 mg, 0.053 mmol) and 3-(diethylamino)propionic acid hydrochloride (17 mg, 0.096 mmol) in CH_2Cl_2 (1 mL) was added HOBt (14 mg, 0.11 mmol) and EDCI (21 mg, 0.11 mmol), and the resulting mixture was stirred at rt for 4 h. It was concentrated under reduced pressure and purified by preparative HPLC to furnish **21l** (15 mg; yield, 55%; mixture of *trans*/*cis* 85:15 by NMR) as a pale yellow solid. LC-MS (ESI positive mode) *m*/*z* 502 ($[M + H]^+$). ^{1}H NMR (MeOD-d_4): δ 8.50−8.49 (m, 2H), 8.37 (s, 1H), 8.01 (d, 1H), 7.62−7.61 (m, 1H), 7.56 (t, 1H), 7.48−7.47 (m, 1H), 7.42 (d, 1H), 7.28 (s, 1H), 5.95−5.81 (m, 2H), 4.64 (s, 2H), 4.59 (s, 2H), 4.17 (d, 2H), 4.10 (d, 2H), 3.55 (t, 2H), 3.34 (q, 4H), 2.94 (t, 2H), 1.40 (t, 6H).

Enzyme Assays. The recombinant enzymes (CDK2/CyclinA, JAK1, JAK2, JAK3 and FLT3) were prepared by the S*BIO biochemistry group according to published procedures. All assays were carried out in 384-well white microtiter plates using the PKLight assay system from Cambrex. This assay platform is essentially a luminometric assay for the detection of ATP in the reaction using a luciferase-coupled reaction. The compounds were tested at 8 concentrations prepared from 3- or 4-fold serial dilution starting at 10 μM. For the CDK2/cyclin A assay, the reaction mixture consisted of the following components in 25 μL assay buffer (50 mM Hepes, pH 7.5, 10 mM $MgCl_2$, 5 mM $MnCl_2$, 5 mM BGP, 1 mM DTT, and 0.1 mM sodium orthovanadate), 1.4 μg/mL of CDK2/cyclin A complex, 0.5 μM of RbING substrate (Invitrogen, cat # PV2939), and 0.5 μM of ATP. The reaction was incubated at room temperature for 2 h. Thirteen microliters of PKLight ATP detection reagent was added, and the reaction was incubated for 10 min. Luminescence signals were detected on a multilabel plate reader (Victor^2 V 1420, Perkin-Elmer). The other kinase assays were similar, with the following differences in reagents. For FLT3 assays, the reaction contained 2.0 μg/mL FLT3 enzyme, 5 μM of poly(Glu,Tyr) substrate (Sigma, cat # P0275), and 4 μM of ATP. For JAK1 assays, the reaction contained 2.5 μg/mL of JAK1 enzyme, 10 μM of poly(Glu,Ala,Tyr) substrate (Sigma, cat # P3899), and 1.0 μM of ATP. For JAK2 assays, the reaction contained 0.35 μg/mL of JAK2 enzyme, 10 μM of poly(Glu, Ala,Tyr) substrate (Sigma, cat # P3899), and 0.15 μM of ATP. For JAK3 assays, the reaction contained 3.5 μg/mL of JAK3 enzyme, 10 μM of poly(Glu,Ala,Tyr) substrate (Sigma, cat # P3899), and 6.0 μM of ATP. The analytical software, Prism 5.0 (GraphPad Software Pte Ltd.) was used to generate IC_{50} values from the data.

Cell Proliferation Assays. Ba/F3-JAK2^{V617F}-GFP-Luc cells were generous gifts from Dr. Martin Sattler (Dana-Farber Cancer Institute, Boston, MA). The generation and culture of these cells has been described previously {Walz, 2006 #2}. MV4−11 cells was obtained from the American Type Culture Collection (ATCC, Manassas, VA) and cultured according to the recommended guidelines. For proliferation assays in 96-well plates, 20.000 cells were seeded in 100 μL and treated the following day with compounds (in triplicates) at concentrations up to 10 μM for 48 h. Cell viability was monitored using the CellTiter-Glo cell proliferation assay (Promega, Madison, WI). Dose−response curves were plotted to determine IC_{50} values for the compounds using the XL-fit software (IDBS Ltd., Alameda, CA).

Allograft Studies with Ba/F3-JAK2^{V617F} Cells. All mice were obtained from the Biological Resource Centre (Biopolis, Singapore). Female athymic BALB/c nude mice (BALB/cOlaHsd-*Foxn1*^{nu}) were 12 weeks of age; female SCID Beige mice (CB17.Cg-*Prkdc*^{scid}*Lyst* ^{bg}/Crl) werr 9−10 weeks of age. Standard protocols were followed, in compliance with the NIH and National Advisory Committee for Laboratory Animal Research guidelines (IACUC approval #0800371).

For the mouse model of MPD, 2×10^6 Ba/F3-JAK2^{V617F} cells were resuspended in 100 μL serum-free culture medium and injected intravenously into the tail vein of BALB/c nude mice. Treatment was started on day 4 for 13 consecutive days for three groups of 8 mice each. Four naïve mice served to establish baseline values. Animals were sacrificed at the end of study, and the spleens and livers were harvested and weighed.

Xenograft Studies with MV4−11 Cells. Female BALB/c mice and female athymic BALB/c nude mice (BALB/cOlaHsd-*Foxn1*^{nu}) were obtained from the Biological Resource Centre (BRC, Biopolis, Singapore) and were 9−16 weeks of age at the time of tumor implantation. Standard protocols were followed, in compliance with the National Institutes of Health and National Advisory Committee for Laboratory Animal Research guidelines (IACUC approval #0800371). Female BALB/c nude mice were implanted subcutaneously in the right flank with 1×10^7 MV4−11 human AML cells. Cells were resuspended in 50 μL of serum-free growth medium, mixed 1:1 with Matrigel

(Cat. No:354248; BD Bioscience), and injected in a total volume of 100 μL, using a 23-gauge needle. MV4−11 tumor-bearing mice (average starting tumor size of 130 mm^3) were treated orally (p.o.) once daily at doses of 25, 50, or 100 mg/kg for 21 consecutive days. After termination of the treatment, tumor growth was measured up to day 55, and the median time to end point (TTE) (median survival) was calculated. End point of experiment for an individual mouse was reached either on day 55 or when a tumor reached a size of 1000 mm^3. The tumor volumes were calculated using the formula: Tumor volume (mm^3) = $(w^2 \times l)/2$ (w = width, and l = length in mm of the tumor xenograft). All doses for in vivo experiments used in this article are given as free base equivalent.

Metabolic Stability in Liver Microsomes. Test compounds (5 μM) were incubated with MLM, RLM, DLM, and HLM (final microsomal concentration of ∼0.87 mg/mL), in a reaction mix containing 50 mM potassium phosphate buffer (pH 7.4), and a NADPH regeneration system, at 37 °C, in a total reaction volume of 1 mL. Reactions were terminated at 0, 15, 30, 45, and 60 min of incubation with a chilled mixture of acetonitrile and DMSO (80:20), vortexed for 5 min, and centrifuged at 13200 rpm for 15 min at 4 °C, and the supernatants were analyzed by LC/MS/MS. Stability was assessed by plotting the percent of parent compound remaining against time on a log−linear scale and estimating the half-life from the linear portion of the log−linear curve using the first order equation $t_{1/2} = 0.693/k$, where k = slope of the curve (equal to the first order elimination rate constant).

Human in vitro CYP450 Inhibition Assay. Test compounds were incubated (at concentrations of 0.05, 0.25, 0.5, 2.5, 5, and 25 μM in DMSO; final DMSO concentration = 0.35%) with human liver microsomes (0.25 mg/mL for CYP1A and CYP3A4, 0.5 mg/mL for CYP2C19 and CYP2D6, 1 mg/mL for CYP2C9) and NADPH (1 mM) in the presence of the probe substrate ethoxyresorufin (0.5 μM) for 5 min (CYP1A), tolbutamide (120 μM) for 60 min (CYP2C9), mephenytoin (25 μM) for 60 min (CYP2C19), dextromethorphan (5 μM) for 30 min (CYP2D6), and midazolam (2.5 μM) for 5 min (CYP3A4) at 37 °C. The selective inhibitors α-naphthoflavone, sulphaphenazole, tranylcypromine, quinidine, and ketoconazole were used as positive controls for CYP1A, CYP2C9, CYP2C19, CYP2D6, and CYP3A4 inhibitors, respectively. For CYP1A, the reactions were terminated by the addition of methanol, and the formation of the metabolite, resorufin, was monitored by fluorescence (excitation wavelength = 535 nm, and emission wavelength = 595 nm). For the CYP2C9, CYP2C19, CYP2D6, and CYP3A4 incubations, the reactions were terminated by the addition of methanol containing an internal standard. The samples were centrifuged, and the supernatants were combined, for the simultaneous analysis of 4-hydroxytolbutamide, 4-hydroxymephenytoin, dextrorphan, 1-hydroxymidazolam, and the internal standard by LC-MS/MS. Formic acid in deionized water (final concentration = 0.1%) was added to the final sample prior to analysis. A decrease in the formation of the metabolites compared to vehicle control was used to calculate an IC_{50} value (test compound concentration which produces 50% inhibition).

Caco-2 Bidirectional Permeability Assay. Compound **21c** at 5 μM in Hank's balanced salt solution (HBSS), final DMSO concentration less than 1%, was placed in 21−28 day confluent monolayer cells in Transwell assay plates. Both apical and basolateral sides were maintained at pH 7.4. When dosed on the apical side, the permeability in the A→B direction was assessed and when dosed on the basolateral side, the B→A direction was assessed. Both apical and basolateral sides were sampled at 2 h. The concentration of **21c** was determined by LC/MS using a 4-point calibration curve. Atenolol (P_{app} <0.5 × 10^{-6} cm/s), propranolol (15 < P_{app} < 25 × 10^{-6} cm/s), Lucifer Yellow (P_{app} > 0.4 × 10^{-6} cm/s), and digoxin (efflux ratio >3) were used in the quality control of the monolayer batch. The integrity of the monolayer was determined by measuring the pre-experiment TEER (between 450 and 650 Ωcm^2) and using Lucifer Yellow (% efflux ≤0.5). The efflux ratio was defined as the ratio of $P_{app,B\rightarrow A}$ to $P_{app,A\rightarrow B}$.

In Vitro Plasma Protein Binding. Equilibrium dialysis was performed in Micro-Equilibrium Dialyzer (Harvard Apparatus) with a chamber volume of 500 μL (each compartment with a volume of 250 μL). The semipermeable membrane used was rinsed with Milli-Q-water and soaked for 10 min in PBS. Compound **21c** was added to plasma (from mouse, dog and humans) to obtain a final concentration of 1000 ng/mL. The spiked plasma was vortexed, and 250 μL was aliquoted into one chamber of the dialyzer cell. The other chamber was filled with 250 μL of PBS buffer. The assembled cell was placed into a water-bath at 37 °C, and dialysis was performed for 4 h. Following dialysis, 50 μL of PBS dialyzed samples containing free **21c** was transferred into 2 mL Eppendorf tubes in triplicate for extraction. Samples were extracted with 1500 μL of MTBE (methyl tertiary-butyl ether) for 30 min using a mixer at motor speed setting 60 with pulsing. After 30 min, the sample tubes were centrifuged at 4 °C for 10 min at 13,000 rpm in a microcentrifuge. The supernatant (1400 μL) was transferred into fresh 2 mL Eppendorf tubes and dried in SpeedVac at 43 °C for 35 min. The dried samples were reconstituted with 100 μL of methanol/Milli-Q-H_2O (60:40) and analyzed by LC/MS/MS.

Pharmacokinetics. Male BALB/c mice (aged ∼8 weeks and weighing 20−23 g), male Beagle dogs (∼ 6 to7 months of age, weighing 9−11 kg), and male Wistar rats (aged 6−8 weeks, weighing 270 to 325 g) were used in this study. All of the animal studies were performed as per approved internal protocols for animal care and use. The oral doses for mice, dogs, and rats were 30, 3, and 10 mg/kg, respectively. The doses were administered, by gavage, as suspensions (0.5 % methylcellulose and 0.1%tween 80) to mice and rats, and as gelatin capsules (12 Torpac) to dogs. Following oral dosing, serial blood samples were collected (retroorbital plexus in mice, jugular vein in dogs, and superior vena cava in rats) at different time points (0 to 24 h) in tubes containing K_3EDTA as anticoagulant, and centrifuged, the plasma was separated and stored at −70 °C until analysis. Plasma samples were processed and analyzed by LC/MS/MS. Pharmacokinetic parameters were estimated by noncompartmental methods using WinNonlin (ver 5.2, Pharsight, CA)

PAMPA (Parallel Artificial Membrane Permeability Assay). This assay measures the permeability of compounds in a high throughput format. The assay was performed in a 96 well format (Millipore MultiScreen 96 well acceptor plate, Teflon tray, Millipore MultiScreen 0.4 μm PCTE membrane clear base plate, 96 well, surface area = 0.24 cm^2, porosity ∼20%). The final concentration of the compounds in the assay was 1 μM. The artificial membrane in the donor plate was prepared by mixing 5% hexadecane in hexane. The donor plate contained 0.15 mL of 5% DMSO in PBS, and the compound (1 μM) and the acceptor plate had 0.3 mL of 5% DMSO in PBS. The assembled plates were placed in a Ziploc bag with wet C-fold towels to prevent evaporation and incubated for 5 h at room temperature. Following incubation, the donor and acceptor solutions were analyzed by LC/MS/MS, and the apparent permeability coefficient (P_{app}) was estimated.

High Throughput solubility Assay. This assay measures the solubility of a compound in PBS in high throughput mode. The assay was done using 96-well semitransparent PP microplates with V-shaped bottoms (Greiner Bio-one) and 96-well UV transparent microplates (Greiner Bio-One). Compound solutions (250 μM) were prepared in 10 mM phosphate buffer (pH 7.0) containing 20% DMSO in a total volume of 0.2 mL. Plates were placed on a shaker set at 600 rpm for 1.5 h, following which the plates were allowed to stand for 2 h at room temperature. The plates were centrifuged at 1500g for 15 min. The supernatants were transferred to a UV transparent microplate and analyzed by UV-spectrophotometry at the appropriate absorption maxima. The concentration of the compound in the supernatant was quantified using a calibration curve. For calculated solubilities of 250 ± 30 μM, solubilities are reported as >250 μM (>150 μg/mL).

Computational. The molecules were built using Maestro 8.0.308 or converted to 3D structures from the 2D structure using LigPrep version 2.1.207.[49] Basic amines were protonated as in the aqueous solution at physiological pH. The conformational space was searched using the Monte Carlo (MCMM) method as implemented in MacroModel version 9.5.207.[49] All heavy atoms and hydrogens on heteroatoms were included in the test for duplicate conformations. All rotatable single bonds were included in the conformational search, and all aliphatic rings were ring-opened, and quaternary atoms were allowed to invert. Each search was continued until the global energy minima were found at least 3 times. The energy minimizations were carried out using the truncated Newton conjugate gradient algorithm (TNCG) and the OPLS-AA force field as implemented in MacroModel.[50] Default parameters were used. The conformational searches were done for aqueous solution using the generalized Born/solvent accessible surface (GB/SA) continuum solvation model.[51]

The JAK1 (PDB entry 3EYG),[52] JAK2 (PDB entry 2B7A),[53] JAK3 (PDB entry 1YVJ),[54] CDK2 (PDB entry 1AQ1),[55] and FLT3 (PDB entry 1RJB)[56] X-ray structures were downloaded from the protein data bank (PDB).[57] The protein structures were prepared using the protein preparation wizard in Maestro with standard settings. Grids were generated using Glide, version 4.5.208, following the standard procedure recommended by Schrödinger.[49] The conformational ensembles were docked flexibly using Glide with standard settings in both standard and extra precision mode. Only poses with low energy conformations and good hydrogen bond geometries were considered. Physical properties were calculated using QikProp, version 3.0.207, with standard settings.[49]

■ ASSOCIATED CONTENT

Supporting Information. Explanation for CDK2 potency of **17h**, Western blots showing intracellular target inhibition by **21c**, and structures of the RCM catalysts employed. This material is available free of charge via the Internet at http://pubs.acs.org.

■ AUTHOR INFORMATION

Corresponding Author

*Tel: (0065) 6827-5021. Fax: (0065) 6827-5005. E-mail: anthony_william@sbio.com.

■ ACKNOWLEDGMENT

We thank Changyong Hu, Bee Kheng Ng, and Yong Cheng Tan for the generation of screening data, Venkatesh Reddy for PK sample analysis, Zahid Bonday and Miah Kiat for protein preparation work, Sam Ramanujulu Murugappan for NMR related work, and Dr. Simon Campbell for helpful discussions.

■ ABBREVIATIONS USED

JAK2, Janus kinase 2; FLT3, fms-like receptor tyrosine kinase 3; RTKs, receptor tyrosine kinases; MF, myelofibrosis; MPN, myeloproliferative neoplasms; PV, polycythemia vera; ET, essential thrombocythemia; STAT, signal transducers and activators of transcription; CYP, cytochrome P450; RCM, ring closing metathesis; SOCS-1 gene, suppressor of cytokine signaling; TYK2, nonreceptor tyrosine kinase 2; ADME, aborption, distribution, metabolism, and elimination

■ REFERENCES

(1) Yamaoka, K.; Saharinen, P.; Pesu, M.; Holt, V. E. T., III; Silvennoinen, O.; O'Shea, J. J. The Janus kinases (Jaks). *Genome Biol.* **2004**, *5*, 253.1–253.6.

(2) Rane, S. G.; Reddy, E. P. Janus kinases: components of multiple signaling pathways. *Oncogene* **2000**, *19*, 5662–5679.

(3) Levine, R. L. Mechanisms of mutations in myeloproliferative neoplasms. *Best Pract. Res. Clin. Haematol.* **2009**, *22*, 489–494.

(4) Levine, R. L.; Wadleigh, M.; Cools, J.; Ebert, B. L.; Wernig, G.; Huntly, B. J. P.; Boggon, T. J.; Wlodarsaka, I.; Clark, J. J.; Moore, S.; Adelsperger, J; Koo, S.; Lee, J. C.; Gabriel, S.; Mercher, T.; D'Andrea, A.; Frohling, S.; Dohner, K.; Marynen, P.; Vandenberghe, P.; Mesa, R. A.; Tefferi, A.; Griffin, J. D.; Eck, M. J.; Sellers, W. R.; Meyerson, M.; Golub, T. R.; Lee, S. J.; Gilliland, D. G. Activating mutation in the tyrosine kinase JAK2 in polycythemia vera, essential thrombocythemia, and myeloid metaplasia with myelofibrosis. *Cancer Cell* **2005**, *7*, 387–397.

(5) Baxter, E. J.; Scott, L. M.; Campbell, P. J.; East, C.; Fourouclas, N.; Swanton, S.; Vassiliou, G. S.; Bench, A. J.; Boyd, E. M.; Curtin, N.; Scott, M. A.; Erber, W. N. Green, A. R. Acquired mutation of the tyrosine kinase JAK2 in human myeloproliferative disorders. *Lancet* **2005**, *365*, 1054–1061.

(6) James, C.; Ugo, V.; Le Couédic, J. P.; Staerk, J.; Delhommeau, F.; Lacout, C.; Garçon, L.; Raslova, H.; Berger, R.; Bennacaur-Griscelli, A.; Villeval, J. L.; Constantinescu, S. N.; Casadevall, N.; Vainchenker, W. A unique clonal JAK2 mutation leading to constitutive signaling causes polycythemia vera. *Nature* **2005**, *434*, 1144–1148.

(7) Tefferi, A. *JAK* and *MPL* mutations in myeloid malignancies. *Leuk. Lymphoma* **2008**, *49*, 388–397.

(8) Gangat, N.; Caramazza, D.; Vaidya, R.; George, G.; Begna, K.; Schwager, S.; Van Dyke, D.; Hanson, C.; Wu, W.; Pardanani, A.; Cervantes, F.; Passamonti, F. DIPSS plus: A refined dynamic international prognostic scoring system for primary myelofibrosis that incorporates prognostic information from karyotype, platelet count, and transfusion status. *J. Clin. Oncol.* **2010**, *32*, 2446.

(9) Purandare, A. V.; Lorenzi, M. V.; Lombardo, L. J. Janus kinase 2 (JAK2) inhibitors for the treatment of myeloproliferative neoplasms (MPN). *Ann. Rep. Med. Chem.* **2010**, *45*, 210–227.

(10) Verstovsek, S.; Kantarjian, H.; Mesa, R. A.; Pardanani, A. D.; Cortes-Franco, J.; Thomas, D. A.; Estrov, Z.; Fridman, J. S.; Bradley, E. C.; Erickson-Viitanen, S.; Vaddi, K.; Levy, R.; Tefferi, A. Safety and efficacy of INCB018424, a JAK1 and JAK2 inhibitor, in myelofibrosis *N. Engl. J. Med.* **2010**, *363*, 1117–1127.

(11) Verstovsek, S. Therapeutic potential of JAK2 inhibitors. *Hematol. Am. Soc. Hematol. Educ. Prog.* **2009**, 636–642.

(12) Santos, F. P.; Verstovsek, S. JAK2 inhibitors: What's the true therapeutic potential? *Blood Rev.* **2011**, *25*, 53–63.

(13) Verstovsek, S.; Odenike, O.; Scott, B.; Estrov, Z.; Cortes, J.; Thomas, D. A.; Wood, J.; Ethirajulu, K.; Lowe, A.; Zhu, H. J.; Kantarjian, H.; Deeg, H. J. Phase I dose escalation trial of SB1518, a novel JAK2/FLT3 inhibitor, in acute and chronic myeloid diseases, including primary or post-essential thrombocythemia/polycythemia vera myelofibrosis. *Blood* **2009**, *114*, Abstr. 3905.

(14) Verstovsek, S.; Deeg, H. J.; Odenike, O.; Zhu, H. J.; Kantarjian, H.; Estrov, Z.; Scott, B.; Cortes, J.; Thomas, D. A. Phase 1/2 study of SB1518, a novel JAK2/FLT3 inhibitor, in the treatment of primary myelofibrosis. *Blood* **2010**, *116*, Abstr. 3082.

(15) Blanchard, S.; Lee, A. C.-H.; Nagaraj, H. K.-M.; Poulsen, A.; Sun, E. T.; Tan, E. Y.-L.; William, A. D. Oxygen linked pyrimidine derivavtives. WO 2007/058627 A, 2007.

(16) Weniger, M. A.; Melzner, I.; Menz, C. K.; Wegener, S.; Bucur, A. J.; Dorsch, K.; Mattfeldt, T.; Barth, T. F. E.; Moller, P. Mutations of the tumor suppressor gene *SOCS-1* in classical Hodgkin lymphoma are frequent and associated with nuclear phospho-STAT5 accumulation. *Oncogene* **2006**, *25*, 2679–2684.

(17) Navarro, A.; Diaz, T.; Martinez, A.; Gaya, A.; Pons, A.; Gel, B.; Codony, C.; Ferrer, G.; Martinez, C.; Montserrat, E.; Monzo, M. Regulation of JAK2 by miR-135a: prognostic impact in classic Hodgkin lymphoma. *Blood* **2009**, *114*, 2945–2951.

(18) Raia, V.; Schilling, M.; Böhm, M.; Hahn, B.; Kowarsch, A.; Raue, A.; Sticht, C.; Bohl, S.; Saile, M.; Möller, P.; Gretz, N.; Timmer, J.; Theis, F.; Lehmann, W.-D.; Lichter, P.; Klingmüller, U. Dynamic mathematical modeling of IL13-induced signaling in hodgkin and primary mediastinal B-cell lymphoma allows prediction of therapeutic targets. *Cancer Res.* **2011**, *71*, 693–704.

(19) Hart, S.; Goh, K. C.; Novotny-Diermayr, V.; Hu, C. Y.; Hentze, H.; Tan, Y. C.; Madan, B.; Amalini, C.; Loh, Y. K.; Ong, L. C.; William, A.; Lee, A.; Poulsen, A.; Jayaraman, R.; Ethirajulu, K.; Dymock, B.; Wood, J. SB1518, a novel macrocyclic pyrimidine-based JAK2 inhibitor for the treatment of myeloid and lymphoid malignancies. *Leukemia* **2011**, in press.

(20) Fridman, J. S.; Scherle, P. A.; Collins, R.; Burn, T. C.; Li, Y.; Li, J.; Covington, M. B.; Thomas, B.; Collier, P.; Favata, M. F.; Wen, X.; Shi., J.; McGee, R.; Haley, P. J.; Shepard, S.; Rodgers, J. D.; Yeleswaram, S.; Hollis, G.; Newton, R. C.; Metcalf, B.; Friedman, S. M.; Vaddi, K. Selective inhibition of JAK1 and JAK2 is efficacious in rodent models of arthritis: preclinical characterization of INCB028050. *J. Immunol.* **2010**, *184*, 5298–307.

(21) Mesa, R. A. Ruxolitinib, a selective JAK1 and JAK2 inhibitor for the treatment of myeloproliferative neoplasms and psoriasis. *IDrugs.* **2010**, *13*, 394–403.

(22) Nosaka, T.; van Deursen, J. M.; Tripp, R. A.; Thierfelder., W. E.; Witthuhn, B. A.; McMickle, A. P.; Doherty, P. C.; Grosveld, G. C.; Ihle, J. N. Defective lymphoid development in mice lacking Jak3. *Science* **1995**, *270*, 800–802.

(23) Gilliland, D. G. FLT3-activating mutations in acute promyelocytic leukaemia: a rationale for risk-adapted therapy with FLT3 inhibitors. *Best Prac. Res. Clin. Haematol.* **2003**, *16*, 409–417.

(24) Naoe, T.; Kiyoi, H. Oncogenic protein kinases: normal and oncogenic FLT3. *Cell. Mol. Life Sci.* **2004**, *61*, 2932–2938.

(25) Kottaridis, P. D.; Gale, R. E.; Linch, D. C. Prognostic implications of the presence of FLT3 mutations in patients with acute myeloid leukemia. *Leuk. Lymphoma* **2003**, *44*, 905–913.

(26) Reilly, J. T. FLT3 and its role in the pathogenesis of acute myeloid leukaemia. *Leuk. Lymphoma* **2003**, *44*, 1–7.

(27) Gilliland, D. G.; Griffin, J. D. Role of FLT3 in leukemia. *Curr. Opin. Hematol.* **2002**, *9*, 274–281.

(28) Younes, A.; Fanale, M. A.; McLaughlin, P.; Copeland, A.; Zhu, J.; Faria, S. C. Phase 1 study of a novel oral JAK-2 inhibitor SB1518 in patients with relapsed lymphoma: Evidence of clinical and biological activity in multiple lymphoma subtypes. *Blood* **2010**, *116*, Abstr. 2830.

(29) Kiss, R.; Sayeski, P. P.; Keserű, G. M. Recent developments on JAK2 inhibitors: a patent review. *Expert Opin. Ther. Pat.* **2010**, *20*, 471–495.

(30) Grubbs, R. H. *Handbook of Metathesis*; Wiley- VCH: New York, 2003; Vols. 1−3.

(31) Quincheng, M.; Manfred, H. Ring closure methods in the synthesis of macrocyclic natural products. *Top. Curr. Chem.* **1992**, *161*, 107–176.

(32) Deiters, A.; Martin, S. F. Synthesis of oxygen- and nitrogen-containing heterocycles by ring-closing metathesis. *Chem. Rev.* **2004**, *104*, 2199–2238.

(33) Tsantrizos, Y. S.; Bolger, G.; Bonneau, P.; Cameron, D. R.; Goudreau, N.; Kukolj, G.; LaPlante, S. R.; Llinàs-Brunet, M.; Nar, H.; Lamarre, D. Macrocyclic inhibitors of the NS3 protease as potential therapeutic agents of hepatitis C virus infection. *Angew. Chem., Int. Ed.* **2003**, *42*, 1356–1360.

(34) Graziani, E. I. Recent advances in the chemistry, biosynthesis and pharmacology of rapamycin analogs. *Nat. Prod. Rep.* **2009**, *26*, 602–609.

(35) Driggers, E. M.; Hale, S. P.; Lee, J.; Terret, N. K. The exploration of macrocycles for drug discovery—an underexploited structural class. *Nat. Rev. Drug Discovery* **2008**, *7*, 608–624.

(36) Joshi, S.; Maikap, G. C.; Titirmare, S.; Chaudhari, A.; Gurjar, M. K. An improved synthesis of etravirine. *Org. Proc. Res. Dev.* **2010**, *14*, 657–660.

(37) Schmidt, B. Ruthenium-catalyzed cyclizations: more than just olefin metathesis! *Angew. Chem., Int. Ed.* **2003**, *42*, 4996–4999.

(38) Cai, Q.; Zhao, Z.-A.; You, S.-L. Asymmetric construction of polycyclic indoles through olefin cross- metathesis/intramolecular Friedel−Crafts alkylation under sequential catalysis. *Angew. Chem., Int. Ed.* **2009**, *48*, 7428–7431.

(39) Suzuki, A. Synthetic studies via the cross-coupling reaction of organoboron derivatives with organic halides. *Pure Appl. Chem.* **1991**, *63*, 419–422.

(40) Miyaura, N.; Suzuki, A. Palladium-catalyzed cross-coupling reactions of organoboron compounds. *Chem. Rev.* **1995**, *95*, 2457–2483.

(41) Rao, P. S-H.; Senthilkumar, S. P. A convenient procedure for the synthesis of allyl and benzyl ethers from alcohols and phenols. *Proc. Indian Acad. Sci.* **2001**, *113*, 191–196.

(42) Koehling, P.; Schmidt, A. M.; Eilbracht, P. Tandem hydroformylation/Fischer indole synthesis: a novel and convenient approach to indoles from olefins. *Org. Lett.* **2003**, *5*, 3213–3216.

(43) Ramadas, K.; Srinivasan, N. Iron-ammonium chloride: a convenient and inexpensive reductant. *Synth. Commun.* **1992**, *22*, 3189–3195.

(44) Hardcastle, I. R.; Rowlands, M. G.; Houghton, J.; Parr, I. B.; Potter, G. A.; Jarman, M.; Edwards, K. J.; Laughton, C. A.; Trent, J. O.; Neidle, S. Rationally designed analogs of tamoxifen with improved calmodulin antagonism. *J. Med. Chem.* **1995**, *38*, 241–248.

(45) Dodge, J. A.; Stocksdale, M. G.; Fahey, K. J.; Jones, C. D. Regioselectivity in the alkaline thiolate deprotection of aryl methyl ethers. *J. Org. Chem.* **1995**, *60*, 739–741.

(46) Niu, C.; Boschelli, D. H.; Tumey, L. N.; Bhagirath, N.; Subrath, J.; Shim, J.; Wang, Y.; Wu, B.; Eid, C.; Lee, J.; Yang, X.; Brennan, A.; Chaudhary, D. First generation 5-vinyl-3-pyridinecarbonitrile PKCθ inhibitors. *Bioorg. Med. Chem. Lett.* **2009**, *19*, 5829–5832.

(47) Pardanani, A.; Lasho, T.; Smith, G.; Burns, C. J.; Fantino, E; Tefferi, A. CYT387, a selective JAK1/JAK2 inhibitor: in vitro assessment of kinase selectivity and preclinical studies using cell lines and primary cells from polycythemia vera patients. *Leukemia* **2009**, *23*, 1441–1445.

(48) For latest trials in Myelofibrosis, Advanced Myeloid Malignancies and Advanced Lymphoid Malignancies see http://clinicaltrials.gov.

(49) *Maestro, Ligprep, Macromodel, Glide and QikProp*; Schrodinger, LLC, New York, NY. 2011. http://www.schrodinger.com

(50) Jorgensen, W. L.; Maxwell, D. S.; Tirado-Rives, J. Development and testing of the OPLS all-atom force field on conformational energetics and properties of organic liquids. *J. Am. Chem. Soc.* **1996**, *118*, 11225–11236.

(51) Hasel, W.; Hendrickson, T. F.; Still, W. C. A rapid approximation to the solvent accessible surface areas of atoms. *Tetrahedron Comput. Method* **1988**, *1*, 103–116.

(52) Williams, N. K.; Bamert, R. S.; Patel, O.; Wang, C.; Walden, P. M.; Wilks, A. F.; Fantino, E.; Rossjohn., J.; Lucet, I. S. Dissecting specificity in the Janus kinases: the structures of JAK-specific inhibitors complexed to the JAK1 and JAK2 protein tyrosine kinase domains. *J. Mol. Biol.* **2009**, *387*, 219–232.

(53) Lucet, I. S.; Fantino, E.; Styles, M.; Bamert, R.; Patel, O.; Broughton, S. E.; Walter, M.; Burns, C. J.; Treutlein, H.; Wilks, A. F.; Rossjohn, J. The structural basis of Janus kinase 2 inhibition by a potent and specific pan-Janus kinase inhibitor. *Blood* **2006**, *107*, 176–183.

(54) Boggon, T. J.; Li, Y.; Manley, P. W.; Eck, M. J. Crystal structure of the JAK3 kinase domain in complex with a staurosporine analog. *Blood* **2005**, *106*, 996–1002.

(55) Lawrie, A. M.; Noble, M. E. M.; Tunnah, P.; Brown, N. R.; Johnson, L. A.; Endicott, J. A. Protein kinase inhibition by staurosporine revealed in details of the molecular interaction with CDK2. *Nat. Struct. Biol.* **1997**, *4*, 796–801.

(56) Griffith, J.; Black, J.; Faerman, C.; Swenson, L.; Wynn, M.; Lu, F.; Lippke, J.; Saxena, K. The structural basis for autoinhibition of FLT3 by the juxtamembrane domain. *Mol. Cell* **2004**, *13*, 169–178.

(57) Berman, H. M.; Westbrook, J.; Feng, Z.; Gilliland, G.; Bhat, T. N.; Weissig, H.; Shindyalov, I. N.; Bourne, P. E. The Protein Data Bank. *Nucleic Acids Res.* **2000**, *28*, 235–242.